

Vacuum Induced CP Violation Generating a Complex CKM Matrix with Controlled Scalar FCNC

Miguel Nebot ^{a,1} Francisco J. Botella ^{b,2}, Gustavo C. Branco ^{a,3},

^a *Departamento de Física and Centro de Física Teórica de Partículas (CFTP), Instituto Superior Técnico (IST), U. de Lisboa (UL), Av. Rovisco Pais 1, P-1049-001 Lisboa, Portugal.*

^b *Departament de Física Teòrica and Instituto de Física Corpuscular (IFIC), Universitat de València – CSIC, E-46100 Valencia, Spain.*

Abstract

We propose a viable minimal model with spontaneous CP violation in the framework of a Two Higgs Doublet Model. The model is based on a generalised Branco-Grimus-Lavoura model with a flavoured \mathbb{Z}_2 symmetry, under which two of the quark families are even and the third one is odd. The lagrangian respects CP invariance, but the vacuum has a CP violating phase, which is able to generate a complex CKM matrix, with the rephasing invariant strength of CP violation compatible with experiment. The question of scalar mediated flavour changing neutral couplings is carefully studied. In particular we point out a deep connection between the generation of a complex CKM matrix from a vacuum phase and the appearance of scalar FCNC. The scalar sector is presented in detail, showing that the new scalars are necessarily lighter than 1 TeV. A complete analysis of the model including the most relevant constraints is performed, showing that it is viable and that it has definite implications for the observation of New Physics signals in, for example, flavour changing Higgs decays or the discovery of the new scalars at the LHC. We give special emphasis to processes like $t \rightarrow hc, hu$, as well as $h \rightarrow bs, bd$, which are relevant for the LHC and the ILC.

¹miguel.r.nebot.gomez@tecnico.ulisboa.pt

²Francisco.J.Botella@uv.es

³gbranco@tecnico.ulisboa.pt

1 Introduction

The first model of spontaneous T and CP violation was proposed [1] by T.D. Lee in 1973 at a time when only two incomplete quark generations were known. The main motivation for Lee's seminal work was to put the breaking of CP and T on the same footing as the breaking of gauge symmetry. In Lee's model, the Lagrangian is CP and T invariant, but the vacuum violates these discrete symmetries. This was achieved through the introduction of two Higgs doublets, with vacuum expectation values with a relative phase which violates T and CP invariance. In Lee's model, CP violation would arise solely from Higgs exchange, since at the time only two generations were known and therefore the CKM matrix was real. The general two Higgs Doublet Model (2HDM) [2,3] has Scalar Flavour Changing Neutral Couplings (SFCNC) at tree level which need to be controlled in order to conform to the stringent experimental constraints. This can be achieved by imposing Natural Flavour Conservation (NFC) in the scalar sector, as suggested by Glashow and Weinberg (GW) [4]. Alternatively, it was suggested by Branco, Grimus and Lavoura (BGL) [5] that one may have 2HDM with tree level SFCNC but with their flavour structure only dependent on the CKM matrix V .

BGL models have been extensively analysed in the literature [6–11], and their phenomenological consequences have been studied, in particular in the context of LHC. Recently BGL models have been generalised [12] in the framework of 2HDM. Both the GW and the BGL schemes can be implemented through the introduction of extra symmetries in the 2HDM. On the other hand, it has been shown [13] that the introduction of these symmetries in the 2HDM prevents the generation of either spontaneous or explicit CP violation in the scalar sector, unless they are softly broken [14]. It was recently discussed [15] that for a scalar potential with an extra symmetry beyond gauge symmetry, there is an intriguing correlation between the capability of the potential to generate explicit and spontaneous CP violation.

In this paper we propose a realistic model of spontaneous CP violation in the framework of 2HDM. At this stage it is worth recalling the obstacles which have to be surmounted by any model of spontaneous CP violation:

- (i) The scalar potential should be able to generate spontaneous CP breaking by a phase of the vacuum, denoted θ .
- (ii) The phase θ should be able to generate a complex CKM matrix, with the strength of CP violation compatible with experiment. Recall that the CKM matrix has to be complex even in the presence of New Physics [16].
- (iii) SFCNC effects should be under control so that they do not violate experimental bounds.

The paper is organised as follows. In the next section we present the structure of the model and specify the flavoured symmetry introduced. In the third section we show how a complex CKM matrix is generated from the vacuum phase. Section 4 contains a detailed analysis of the scalar potential with real couplings. In section 5 we derive the

physical Yukawa couplings and the phenomenological analysis of the model is presented in section 6. Finally we present our conclusions in the last section.

2 The Structure of the Model and the Flavoured symmetry

The Yukawa couplings in the 2HDM read

$$\mathcal{L}_Y = -\bar{Q}_L^0(\Gamma_1\Phi_1 + \Gamma_2\Phi_2)d_R^0 - \bar{Q}_L^0(\Delta_1\tilde{\Phi}_1 + \Delta_2\tilde{\Phi}_2)u_R^0 + \text{H.c.}, \quad (1)$$

with summation over generation indices understood and $\tilde{\Phi}_j = i\sigma_2\Phi_j^*$. We consider the following \mathbb{Z}_2 transformations to define the model:

$$\begin{aligned} \Phi_1 &\mapsto \Phi_1, & \Phi_2 &\mapsto -\Phi_2, & Q_{L3}^0 &\mapsto -Q_{L3}^0, & Q_{Lj}^0 &\mapsto Q_{Lj}^0, & j &= 1, 2, \\ d_{Rk}^0 &\mapsto d_{Rk}^0, & u_{Rk}^0 &\mapsto u_{Rk}^0, & k &= 1, 2, 3. \end{aligned} \quad (2)$$

Invariance under eq. (2) gives the following form of the Yukawa coupling matrices:

$$\begin{aligned} \Gamma_1 &= \begin{pmatrix} \times & \times & \times \\ \times & \times & \times \\ 0 & 0 & 0 \end{pmatrix}, & \Gamma_2 &= \begin{pmatrix} 0 & 0 & 0 \\ 0 & 0 & 0 \\ \times & \times & \times \end{pmatrix}, \\ \Delta_1 &= \begin{pmatrix} \times & \times & \times \\ \times & \times & \times \\ 0 & 0 & 0 \end{pmatrix}, & \Delta_2 &= \begin{pmatrix} 0 & 0 & 0 \\ 0 & 0 & 0 \\ \times & \times & \times \end{pmatrix}. \end{aligned} \quad (3)$$

The symmetry assignment in eq. (2) and the Yukawa matrices in eq. (3) correspond to the generalised BGL models introduced in [12]. We impose CP invariance at the Lagrangian level, so we require the Yukawa couplings to be real:

$$\Gamma_j^* = \Gamma_j, \quad \Delta_j^* = \Delta_j. \quad (4)$$

We write the scalar doublets Φ_j in the ‘‘Higgs basis’’ $\{H_1, H_2\}$ [17–19] (see section 4 and appendix B for further details on the scalar sector)

$$\begin{pmatrix} H_1 \\ H_2 \end{pmatrix} = \mathcal{R}_\beta \begin{pmatrix} e^{-i\theta_1}\Phi_1 \\ e^{-i\theta_2}\Phi_2 \end{pmatrix}, \quad \text{with} \quad \mathcal{R}_\beta = \begin{pmatrix} c_\beta & s_\beta \\ -s_\beta & c_\beta \end{pmatrix}, \quad \mathcal{R}_\beta^T = \mathcal{R}_\beta^{-1}. \quad (5)$$

In this basis, only H_1 acquires a vacuum expectation value

$$\langle H_1 \rangle = \frac{v}{\sqrt{2}} \begin{pmatrix} 0 \\ 1 \end{pmatrix}, \quad \langle H_2 \rangle = \begin{pmatrix} 0 \\ 0 \end{pmatrix}. \quad (6)$$

Equation (1) can then be rewritten as

$$\mathcal{L}_Y = -\frac{\sqrt{2}}{v}\bar{Q}_L^0(M_d^0H_1 + N_d^0H_2)d_R^0 - \frac{\sqrt{2}}{v}\bar{Q}_L^0(M_u^0\tilde{H}_1 + N_u^0\tilde{H}_2)u_R^0 + \text{H.c.}, \quad (7)$$

where the quark mass matrices M_d^0 , M_u^0 and the N_d^0 , N_u^0 matrices read

$$M_d^0 = \frac{ve^{i\theta_1}}{\sqrt{2}}(c_\beta\Gamma_1 + e^{i\theta}s_\beta\Gamma_2), \quad N_d^0 = \frac{ve^{i\theta_1}}{\sqrt{2}}(-s_\beta\Gamma_1 + e^{i\theta}c_\beta\Gamma_2), \quad (8)$$

$$M_u^0 = \frac{ve^{-i\theta_1}}{\sqrt{2}}(c_\beta\Delta_1 + e^{-i\theta}s_\beta\Delta_2), \quad N_u^0 = \frac{ve^{-i\theta_1}}{\sqrt{2}}(-s_\beta\Delta_1 + e^{-i\theta}c_\beta\Delta_2), \quad (9)$$

where $\theta = \theta_2 - \theta_1$ is the relative phase among $\langle\Phi_2\rangle$ and $\langle\Phi_1\rangle$. For simplicity, we remove the irrelevant global phases $e^{\pm i\theta_1}$ setting $\theta_1 = 0$.

Notice that the matrices N_d^0 , N_u^0 can be written:

$$N_d^0 = t_\beta M_d^0 + e^{i\theta} \frac{v}{\sqrt{2}}(t_\beta + t_\beta^{-1})s_\beta\Gamma_2 = t_\beta M_d^0 - (t_\beta + t_\beta^{-1})P_3 M_d^0, \quad (10)$$

$$N_u^0 = t_\beta M_u^0 + e^{-i\theta} \frac{v}{\sqrt{2}}(t_\beta + t_\beta^{-1})s_\beta\Delta_2 = t_\beta M_u^0 - (t_\beta + t_\beta^{-1})P_3 M_u^0, \quad (11)$$

where P_3 is the projector

$$P_3 = \begin{pmatrix} 0 & 0 & 0 \\ 0 & 0 & 0 \\ 0 & 0 & 1 \end{pmatrix}. \quad (12)$$

3 Generation of a complex CKM matrix from the vacuum phase

In this section, we show how the vacuum phase θ is capable of generating a complex CKM matrix. As previously emphasized, this is a necessary requirement for the model to be consistent with experiment. Following eqs. (3)-(4) and (8)-(9), we write:

$$M_d^0 = \begin{pmatrix} 1 & 0 & 0 \\ 0 & 1 & 0 \\ 0 & 0 & e^{i\theta} \end{pmatrix} \hat{M}_d^0, \quad M_u^0 = \begin{pmatrix} 1 & 0 & 0 \\ 0 & 1 & 0 \\ 0 & 0 & e^{-i\theta} \end{pmatrix} \hat{M}_u^0, \quad (13)$$

with \hat{M}_d^0 and \hat{M}_u^0 *real*. Then,

$$M_d^0 M_d^{0\dagger} = \begin{pmatrix} 1 & 0 & 0 \\ 0 & 1 & 0 \\ 0 & 0 & e^{i\theta} \end{pmatrix} \hat{M}_d^0 \hat{M}_d^{0T} \begin{pmatrix} 1 & 0 & 0 \\ 0 & 1 & 0 \\ 0 & 0 & e^{-i\theta} \end{pmatrix} \quad (14)$$

with $\hat{M}_d^0 \hat{M}_d^{0T}$ *real* and *symmetric*, which is diagonalised with a real orthogonal transformation:

$$\mathcal{O}_L^{dT} \hat{M}_d^0 \hat{M}_d^{0T} \mathcal{O}_L^d = \text{diag}(m_{d_i}^2). \quad (15)$$

Consequently, eq. (14) gives

$$\mathcal{O}_L^{dT} \begin{pmatrix} 1 & 0 & 0 \\ 0 & 1 & 0 \\ 0 & 0 & e^{-i\theta} \end{pmatrix} M_d^0 M_d^{0\dagger} \begin{pmatrix} 1 & 0 & 0 \\ 0 & 1 & 0 \\ 0 & 0 & e^{i\theta} \end{pmatrix} \mathcal{O}_L^d = \text{diag}(m_{d_i}^2). \quad (16)$$

That is, the diagonalisation of $M_d^0 M_d^{0\dagger}$ is accomplished with

$$\mathcal{U}_L^{d\dagger} M_d^0 M_d^{0\dagger} \mathcal{U}_L^d = \text{diag}(m_{d_i}^2), \quad \text{where} \quad \mathcal{U}_L^d = \begin{pmatrix} 1 & 0 & 0 \\ 0 & 1 & 0 \\ 0 & 0 & e^{i\theta} \end{pmatrix} \mathcal{O}_L^d. \quad (17)$$

Similarly,

$$\mathcal{U}_L^{u\dagger} M_u^0 M_u^{0\dagger} \mathcal{U}_L^u = \text{diag}(m_{u_i}^2), \quad \text{with} \quad \mathcal{U}_L^u = \begin{pmatrix} 1 & 0 & 0 \\ 0 & 1 & 0 \\ 0 & 0 & e^{-i\theta} \end{pmatrix} \mathcal{O}_L^u. \quad (18)$$

Notice the important sign difference in θ between eqs. (17) and (18), which give the following CKM matrix $V \equiv \mathcal{U}_L^{u\dagger} \mathcal{U}_L^d$,

$$V = \mathcal{O}_L^{uT} \begin{pmatrix} 1 & 0 & 0 \\ 0 & 1 & 0 \\ 0 & 0 & e^{i2\theta} \end{pmatrix} \mathcal{O}_L^d. \quad (19)$$

Notice also that, if $e^{i2\theta} = \pm 1$, V is real, i.e. it does not generate CP violation. This can be understood through a careful analysis of the potential, which will be presented in section 4. The model we present here has spontaneous CP violation and thus a physical phase in the CKM matrix can only arise from θ . In section 4.1 we show that for $\theta = \pi/2$ the vacuum is CP invariant and no CP violation can be generated in this model. In particular CKM is necessarily real for this value of θ , as noticed in eq. (19).

It is also straightforward to observe that $M_d^{0\dagger} M_d^0$ and $M_u^{0\dagger} M_u^0$ are real and symmetric, and are thus diagonalised with real orthogonal matrices \mathcal{O}_R^d and \mathcal{O}_R^u ,

$$\mathcal{O}_R^{dT} M_d^{0\dagger} M_d^0 \mathcal{O}_R^d = \text{diag}(m_{d_i}^2), \quad \mathcal{O}_R^{uT} M_u^{0\dagger} M_u^0 \mathcal{O}_R^u = \text{diag}(m_{u_i}^2), \quad (20)$$

such that the bi-diagonalisation of M_d^0 and M_u^0 reads

$$M_d = \text{diag}(m_{d_i}) = \mathcal{U}_L^{d\dagger} M_d^0 \mathcal{O}_R^d, \quad M_u = \text{diag}(m_{u_i}) = \mathcal{U}_L^{u\dagger} M_u^0 \mathcal{O}_R^u. \quad (21)$$

Following eq. (10),

$$N_d \equiv \mathcal{U}_L^{d\dagger} N_d^0 \mathcal{O}_R^d = t_\beta \mathcal{U}_L^{d\dagger} M_d^0 \mathcal{O}_R^d - (t_\beta + t_\beta^{-1}) \mathcal{U}_L^{d\dagger} \mathbb{P}_3 M_d^0 \mathcal{O}_R^d = t_\beta M_d - (t_\beta + t_\beta^{-1}) \mathcal{U}_L^{d\dagger} \mathbb{P}_3 \mathcal{U}_L^d M_d, \quad (22)$$

with \mathbb{P}_3 the projector in eq. (12) and \mathcal{U}_L^d in eq. (17). In the last term of eq. (22),

$$\mathcal{U}_L^{d\dagger} \mathbb{P}_3 \mathcal{U}_L^d = \mathcal{O}_L^{dT} \mathbb{P}_3 \mathcal{O}_L^d, \quad (23)$$

that is, N_d in eq. (22) is *real*. Introducing a real unit vector $\hat{r}_{[d]}$ and a complex unit vector $\hat{n}_{[d]}$ with components

$$\hat{r}_{[d]j} \equiv [\mathcal{O}_L^d]_{3j}, \quad \hat{n}_{[d]j} \equiv [\mathcal{U}_L^d]_{3j} = e^{i\theta} \hat{r}_{[d]j}, \quad (24)$$

one has, for $\mathcal{U}_L^{d\dagger} \mathbf{P}_3 \mathcal{U}_L^d$ in eq. (23),

$$[\mathcal{U}_L^{d\dagger} \mathbf{P}_3 \mathcal{U}_L^d]_{ij} = \hat{n}_{[d]i}^* \hat{n}_{[d]j} = \hat{r}_{[d]i} \hat{r}_{[d]j}. \quad (25)$$

Similarly, for N_u we have

$$N_u \equiv \mathcal{U}_L^{u\dagger} N_u^0 \mathcal{O}_R^u = t_\beta M_u - (t_\beta + t_\beta^{-1}) \mathcal{U}_L^{u\dagger} \mathbf{P}_3 \mathcal{U}_L^u M_u, \quad (26)$$

with

$$\mathcal{U}_L^{u\dagger} \mathbf{P}_3 \mathcal{U}_L^u = \mathcal{O}_L^{uT} \mathbf{P}_3 \mathcal{O}_L^u, \quad (27)$$

and

$$\hat{r}_{[u]j} \equiv [\mathcal{O}_L^u]_{3j} \quad \hat{n}_{[u]j} \equiv [\mathcal{U}_L^u]_{3j} = e^{-i\theta} \hat{r}_{[u]j}, \quad [\mathcal{U}_L^{u\dagger} \mathbf{P}_3 \mathcal{U}_L^u]_{ij} = \hat{n}_{[u]i}^* \hat{n}_{[u]j} = \hat{r}_{[u]i} \hat{r}_{[u]j}. \quad (28)$$

Like N_d , N_u is *real*; N_d and N_u have the form:

$$[N_d]_{ij} = t_\beta \delta_{ij} m_{d_i} - (t_\beta + t_\beta^{-1}) \hat{n}_{[d]i}^* \hat{n}_{[d]j} m_{d_j}, \quad (29)$$

$$[N_u]_{ij} = t_\beta \delta_{ij} m_{u_i} - (t_\beta + t_\beta^{-1}) \hat{n}_{[u]i}^* \hat{n}_{[u]j} m_{u_j}. \quad (30)$$

Since $V = \mathcal{U}_L^{u\dagger} \mathcal{U}_L^d$, the complex unitary vectors $\hat{n}_{[d]}$ and $\hat{n}_{[u]}$ are not independent:

$$\hat{n}_{[d]i} = \hat{n}_{[u]j} V_{ji}, \quad \hat{n}_{[u]i} = V_{ij}^* \hat{n}_{[d]j}. \quad (31)$$

It is interesting to notice that the 2HDM scenario studied in [20], where the soft breaking of a \mathbb{Z}_3 symmetry is the source of CP violation, shares some interesting properties with the present one: there, the CKM matrix can also be factorised in terms of real orthogonal rotations and a diagonal matrix containing the CP violating dependence; the tree level SFCNC are also real in that phase convention. Other aspects of the model like the structure of the Yukawa couplings as well as the scalar sector to be discussed in section 4 are, however, completely different.

In the rest of this section, we analyse in detail the generation of a complex CKM matrix from the vacuum phase θ . The couplings of the physical scalars to the fermions are discussed in section 5, after the discussion of the scalar sector in 4.

It is clear that $e^{i2\theta} \neq \pm 1$ is necessary in order to have an irreducibly complex CKM matrix. However, one has to verify that one can indeed obtain a realistic CKM matrix, one that it is in agreement with the experimental constraints on the moduli $|V_{ij}|$ (in particular of the moduli of the first and second rows), and on the CP violating phase $\gamma \equiv \arg(-V_{ud} V_{ub}^* V_{cb} V_{cd}^*)$ (the only one accessible through tree level processes alone). Concerning CP violation, one can alternatively analyse that the unique (up to a sign) imaginary part of a rephasing invariant quartet $\text{Im}(V_{i_1 j_1} V_{i_1 j_2}^* V_{i_2 j_2} V_{i_2 j_1}^*)$ ($i_1 \neq i_2$, $j_1 \neq j_2$) has the correct size $\sim 3 \times 10^{-5}$. Starting with eq. (19), one can compute that imaginary part. For the task, it is convenient to trade \mathcal{O}_L^d and \mathcal{O}_L^u for the real unit vector $\hat{r}_{[d]}$ in eq. (24) and the real orthogonal matrix R :

$$\hat{r}_{[d]j} = [\mathcal{O}_L^d]_{3j}, \quad R \equiv \mathcal{O}_L^{uT} \mathcal{O}_L^d. \quad (32)$$

Then, one can rewrite

$$V = \mathcal{O}_L^{uT} [\mathbf{1} + (e^{i2\theta} - 1)P_3] \mathcal{O}_L^d \Rightarrow V_{ij} = R_{ij} + (e^{i2\theta} - 1)S_{ij}, \quad (33)$$

and we introduce S_{ij} to allow for compact expressions:

$$S_{ij} \equiv [\mathcal{O}_L^{uT} P_3 \mathcal{O}_L^d]_{ij} = \hat{r}_{[u]i} \hat{r}_{[d]j} = \sum_{k=1}^3 R_{ik} \hat{r}_{[d]k} \hat{r}_{[d]j} = \sum_{k=1}^3 \hat{r}_{[u]i} \hat{r}_{[u]k} R_{kj}. \quad (34)$$

The real and imaginary parts of V_{ij} are⁴

$$\text{Re}(V_{ij}) = R_{ij} - 2s_\theta^2 S_{ij}, \quad \text{Im}(V_{ij}) = s_{2\theta} S_{ij}. \quad (35)$$

Notice that, although eq. (35) is not rephasing invariant, this poses no problem when considering rephasing invariant quartets. With eq. (35), one can obtain:

$$\begin{aligned} \text{Im}(V_{i_1 j_1} V_{i_1 j_2}^* V_{i_2 j_2} V_{i_2 j_1}^*) &= \sin 2\theta \left\{ 4s_\theta^2 (R_{i_1 j_1} S_{i_2 j_2} R_{i_2 j_2} S_{i_1 j_2} - S_{i_1 j_1} R_{i_2 j_1} S_{i_2 j_2} R_{i_1 j_2}) + \right. \\ &4s_\theta^2 (S_{i_1 j_1} S_{i_2 j_1} S_{i_2 j_2} R_{i_1 j_2} - S_{i_1 j_1} S_{i_2 j_1} R_{i_2 j_2} S_{i_1 j_2} + S_{i_1 j_1} R_{i_2 j_1} S_{i_2 j_2} S_{i_1 j_2} - R_{i_1 j_1} S_{i_2 j_1} S_{i_2 j_2} S_{i_1 j_2}) \\ &\left. + S_{i_1 j_1} R_{i_2 j_1} R_{i_2 j_2} R_{i_1 j_2} - R_{i_1 j_1} S_{i_2 j_1} R_{i_2 j_2} R_{i_1 j_2} + R_{i_1 j_1} R_{i_2 j_1} S_{i_2 j_2} R_{i_1 j_2} - R_{i_1 j_1} R_{i_2 j_1} R_{i_2 j_2} S_{i_1 j_2} \right\}. \end{aligned} \quad (36)$$

Although eq. (36) is not very illuminating, one can nevertheless illustrate that realistic values of $\text{Im}(V_{i_1 j_1} V_{i_1 j_2}^* V_{i_2 j_2} V_{i_2 j_1}^*)$ can be obtained even in cases with less parametric freedom, as done in subsection 3.3 below. The general case is analysed in subsection 3.4. Before addressing those questions, we discuss two important aspects that deserve attention in the next two subsections: (i) the number of independent parameters and the most convenient choice for them, (ii) the fact that in this model, if tree level SFCNC were completely absent in one quark sector, then the CKM matrix would not be CP violating. One encounters again a deep connection [21] between the complexity of CKM and SFCNC, in the context of models with spontaneous CP violation.

3.1 Parameters

The CKM matrix V requires 4 physical parameters, while the tree level SFCNC require 2, since $\hat{r}_{[d]}$ is a unit real vector. One can parametrise $\hat{r}_{[d]}$ in terms of two angles θ_d , φ_d :

$$\hat{r}_{[d]} = (\sin \theta_d \cos \varphi_d, \sin \theta_d \sin \varphi_d, \cos \theta_d), \quad (37)$$

as shown in Figure 1⁵. The orthogonal matrix R requires 3 real parameters; together with θ and $\hat{r}_{[d]}$, these 6 parameters match the parameters necessary to describe V (4 parameters) and the products $\hat{r}_{[d]j} \hat{r}_{[d]k}$, $\hat{r}_{[u]j} \hat{r}_{[u]k}$ (2 parameters). However, in terms of

⁴Here and in the following $c_x \equiv \cos x$, $s_x \equiv \sin x$.

⁵The different products $\hat{r}_{[d]i} \hat{r}_{[d]j}$ controlling SFCNC are, simply, the areas of the shaded rectangular projections in the (\hat{i}, \hat{j}) planes in Figure 1.

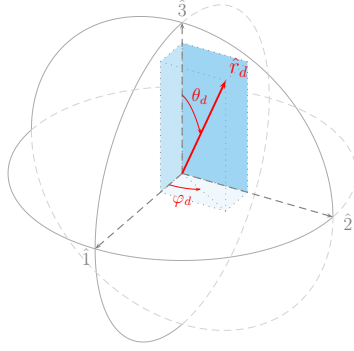


Figure 1: $\hat{r}_{[d]}$.

\mathcal{O}_L^u and \mathcal{O}_L^d , there are a priori 3+3 real parameters; together with θ , 7 parameters in all. This apparent mismatch can be readily understood: a common redefinition

$$\mathcal{O}_L^d \mapsto \begin{pmatrix} \cos \alpha & \sin \alpha & 0 \\ -\sin \alpha & \cos \alpha & 0 \\ 0 & 0 & 1 \end{pmatrix} \mathcal{O}_L^d, \quad \mathcal{O}_L^u \mapsto \begin{pmatrix} \cos \alpha & \sin \alpha & 0 \\ -\sin \alpha & \cos \alpha & 0 \\ 0 & 0 & 1 \end{pmatrix} \mathcal{O}_L^u, \quad (38)$$

leaves R , $\hat{r}_{[d]}$, $\hat{r}_{[u]}$ and V unchanged, effectively removing one parameter from the \mathcal{O}_L^u , \mathcal{O}_L^d , parameter count. Consequently, it is convenient to adopt a parametrisation of R of the form

$$\begin{aligned} R &= \begin{pmatrix} 1 & 0 & 0 \\ 0 & c_{\alpha_3} & s_{\alpha_3} \\ 0 & -s_{\alpha_3} & c_{\alpha_3} \end{pmatrix} \begin{pmatrix} c_{\alpha_2} & 0 & s_{\alpha_2} \\ 0 & 1 & 0 \\ -s_{\alpha_2} & 0 & c_{\alpha_2} \end{pmatrix} \begin{pmatrix} c_{\alpha_1} & s_{\alpha_1} & 0 \\ -s_{\alpha_1} & c_{\alpha_1} & 0 \\ 0 & 0 & 1 \end{pmatrix} \\ &= \begin{pmatrix} c_{\alpha_1} c_{\alpha_2} & s_{\alpha_1} c_{\alpha_2} & s_{\alpha_2} \\ -s_{\alpha_1} c_{\alpha_3} - c_{\alpha_1} s_{\alpha_2} s_{\alpha_3} & c_{\alpha_1} c_{\alpha_3} - s_{\alpha_1} s_{\alpha_2} s_{\alpha_3} & c_{\alpha_2} s_{\alpha_3} \\ s_{\alpha_1} s_{\alpha_3} - c_{\alpha_1} s_{\alpha_2} c_{\alpha_3} & -c_{\alpha_1} s_{\alpha_3} - s_{\alpha_1} s_{\alpha_2} c_{\alpha_3} & c_{\alpha_2} c_{\alpha_3} \end{pmatrix}, \quad (39) \end{aligned}$$

and a parametrisation of \mathcal{O}_L^d of the form⁶

$$\mathcal{O}_L^d = \begin{pmatrix} c_{\alpha} & s_{\alpha} & 0 \\ -s_{\alpha} & c_{\alpha} & 0 \\ 0 & 0 & 1 \end{pmatrix} \begin{pmatrix} c_{\theta_d} c_{\varphi_d} & c_{\theta_d} s_{\varphi_d} & -s_{\theta_d} \\ -s_{\varphi_d} & c_{\varphi_d} & 0 \\ s_{\theta_d} c_{\varphi_d} & s_{\theta_d} s_{\varphi_d} & c_{\theta_d} \end{pmatrix}, \quad (40)$$

where $\hat{r}_{[d]}$ is readily identified in the third row and the redundant α , as in eq. (38), can be set to $\alpha = 0$. One can then concentrate on $\{\alpha_1, \alpha_2, \alpha_3, \theta_d, \varphi_d, \theta\}$ in order to reproduce a realistic CKM matrix.

3.2 SFCNC and CP Violation in CKM

In eqs. (29)–(30), tree level SFCNC are a priori present in both the up and the down quark sectors and controlled by $\hat{n}_{[q]i}^* \hat{n}_{[q]j} = \hat{r}_{[q]i} \hat{r}_{[q]j}$. Therefore, if $\hat{r}_{[q]}$ has a vanishing

⁶The rows in eq. (40) are simply unit vectors in spherical coordinates at $\vec{r} = \hat{r}_{[d]}$, while α , in eq. (40) as in eq. (38), produces an irrelevant rotation around $\hat{r}_{[d]}$.

component, SFCNC in that sector ($q = u$ or d) do only appear in one type of transition (the one not involving that component). If $\hat{r}_{[q]}$ had two vanishing components (then the remaining one equals ± 1), there would not be SFCNC in that sector: interestingly, in this model, having no tree level SFCNC in one quark sector is *incompatible* with a CP violating CKM matrix. This can be readily checked by noticing that, in that case, in eq. (34), the matrix with entries S_{ij} has only a non vanishing row (column), corresponding to the absence of tree level SFCNC in the up (down) sector, for which $S_{ij} = R_{ij}$. Then, with $i_1 \neq i_2$ and $j_1 \neq j_2$, in eq. (36) all terms except two out of the last four automatically vanish, and those two terms appear with opposite sign, giving $\text{Im}(V_{i_1 j_1} V_{i_1 j_2}^* V_{i_2 j_2} V_{i_2 j_1}^*) = 0$. As illustrated below, in subsection 3.4, this implies that a lower bound on the size of the second largest component in $\hat{r}_{[q]}$ should exist, that is a lower bound on the intensity of some SFCNC in both quark sectors. Appendix A completes the discussion of the interplay in this model among flavour non-conservation and CP violation in the CKM matrix.

3.3 A simple example

As a simplified example of how a realistic CKM matrix can be obtained, consider a scenario with

$$\hat{r}_{[d]} = (\cos \varphi_d, \sin \varphi_d, 0). \quad (41)$$

Then, for $i_1 = j_1 = 1$, $i_2 = j_2 = 2$, eq. (36) reduces to

$$\text{Im}(V_{11} V_{12}^* V_{22} V_{21}^*) = \frac{1}{2}(R_{11} R_{21} + R_{12} R_{22})(R_{12} R_{21} - R_{11} R_{22}) \sin 2\varphi_d \sin 2\theta. \quad (42)$$

Since the rows of R form a complete orthonormal set of 3-vectors,

$$R_{11} R_{21} + R_{12} R_{22} = -R_{13} R_{23}, \quad R_{12} R_{21} - R_{11} R_{22} = -R_{33}, \quad (43)$$

and eq. (42) is further reduced to

$$\text{Im}(V_{11} V_{12}^* V_{22} V_{21}^*) = \frac{1}{2} R_{13} R_{23} R_{33} \sin 2\varphi_d \sin 2\theta. \quad (44)$$

With R in eq. (39), eq. (42) gives

$$\text{Im}(V_{11} V_{12}^* V_{22} V_{21}^*) = \frac{1}{8} \cos \alpha_2 \sin 2\alpha_2 \sin 2\alpha_3 \sin 2\varphi_d \sin 2\theta. \quad (45)$$

A complete example of this type which reproduces correctly the CKM matrix, is given by:

$$\theta = \pi/8, \quad (46)$$

$$R = \begin{pmatrix} 1 - 7 \times 10^{-6} & 0 & -3.746 \times 10^{-3} \\ -1.536 \times 10^{-4} & -1 + 8.41 \times 10^{-4} & -0.041 \\ -3.743 \times 10^{-3} & 0.041 & -1 + 8.48 \times 10^{-4} \end{pmatrix}, \quad (47)$$

and

$$\mathcal{O}_L^d = \begin{pmatrix} 0 & 0 & -1 \\ 0.9509 & 0.3096 & 0 \\ 0.3096 & -0.9509 & 0 \end{pmatrix}. \quad (48)$$

The parameters underlying eqs. (47)–(48) have the values

$$\begin{aligned} R : \quad & \alpha_1 = 0, \quad \alpha_2 = -3.746 \times 10^{-3}, \quad \alpha_3 = 0.041 - \pi, \\ \mathcal{O}_L^d : \quad & \theta_d = \pi/2, \quad \varphi_d = -1.2561, \quad \alpha = 0. \end{aligned} \quad (49)$$

For R , $\alpha_1 = 0$ has been chosen for simplicity, since in this scenario it does not enter eq. (45). With the previous values, one can easily check that

$$|V_{us}| = 0.2253, \quad |V_{ub}| = 3.75 \times 10^{-3}, \quad |V_{cb}| = 0.041, \quad \text{Im}(V_{11}V_{12}^*V_{22}V_{21}^*) = 3.195 \times 10^{-5}. \quad (50)$$

Concerning the discussion in subsection 3.2, this example shows that, although the complete absence of tree level FCNC in one sector is incompatible with a CP violating CKM matrix, this incompatibility does not extend to the case of tree level SFCNC circumscribed to only one type of transition (in this example, $d \leftrightarrow s$ transitions).

3.4 General case

The previous example illustrates that the CKM matrix can be adequately reproduced even in a restricted scenario where one has less number of free parameters. For the general case one can explore with a simple numerical analysis the regions of parameter space where the CKM matrix is in agreement with data, that is moduli $|V_{ij}|$ in the first two rows and the phase γ agree with experimental results [22].

Figure 2(a) shows the region of the plane $|\sin 2\theta|$ vs. θ_d which can yield a good CKM matrix. It is to be noticed that (i) regions rather close to $\theta = 0, \pi/2, \pi$, with $|\sin 2\theta| < 10^{-2}$, are allowed and require $\theta_d \sim \pi/4, 3\pi/4$, while (ii) for $|\sin 2\theta| \sim 1$, allowed regions require $\theta_d \sim 0, \pi/2, \pi$. In any case, $\sin 2\theta \neq 0$ is a necessary requirement, as expected, since there is no CP violation in that limit.

Figures 2(d)–2(f) also show the allowed regions in the $\sin \theta_d \sin \varphi_d$ vs. $\sin \theta_d \cos \varphi_d$ plane⁷, separating $|\sin 2\theta| \geq 10^{-1}$ in 2(d), $10^{-1} \geq |\sin 2\theta| \geq 10^{-2}$ in 2(e), and $10^{-2} \geq |\sin 2\theta|$ in 2(f).

Following the discussion in subsection 3.2, one can sort the components of $\hat{r}_{[d]}$ according to their size:

$$|\hat{r}_{[d]Min}| \leq |\hat{r}_{[d]Mid}| \leq |\hat{r}_{[d]Max}|. \quad (51)$$

Incompatibility with a CP violating CKM matrix implies that $|\hat{r}_{[d]Mid}| \neq 0$, while the simple example in subsection 3.3 shows that $|\hat{r}_{[d]Min}| = 0$ is allowed. Figure 2(b) shows the allowed region of $|\hat{r}_{[d]Min}|$ vs. $|\hat{r}_{[d]Mid}|$ confirming that it is necessary that $|\hat{r}_{[d]Mid}| \geq 2 \times 10^{-3}$, while figure 2(c) corresponds similarly to $\hat{r}_{[u]}$: both figures illustrate that, in this model, necessarily, there is at least some minimal presence of tree SFCNC⁸.

In conclusion, it is clear that the first requirement on the model, i.e. that it can reproduce the observed CKM matrix, can be fulfilled.

⁷That is, the projection on the $(\hat{1}, \hat{2})$ plane of the allowed regions in the surface of the sphere of Figure 1.

⁸Notice that, consequently, $\theta_d = 0, \pi$ are excluded: the resolution in Figures 2(a) and 2(d) is too coarse to observe that, while Figures 2(b) and 2(c) clearly illustrate the point.

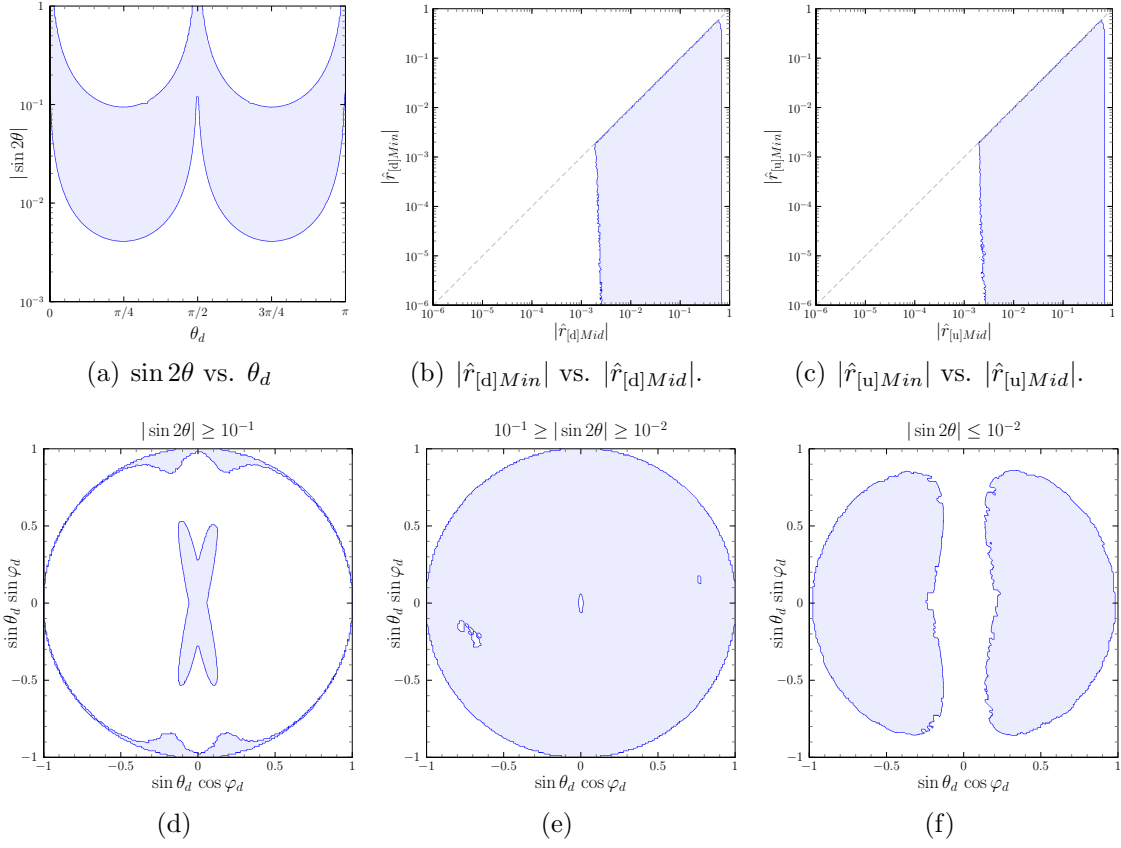


Figure 2: Regions (at 99% C.L.) which reproduce a realistic CKM matrix are shown.

4 The scalar potential with real couplings

We consider the 2HDM with CP invariance and impose the \mathbb{Z}_2 symmetry of eq. (2) which is only softly broken by a μ_{12} term. All couplings are real, so that CP holds at the Lagrangian level. The scalar potential can be written:

$$\begin{aligned} \mathcal{V}(\Phi_1, \Phi_2) = & \mu_{11}^2 \Phi_1^\dagger \Phi_1 + \mu_{22}^2 \Phi_2^\dagger \Phi_2 + \mu_{12}^2 (\Phi_1^\dagger \Phi_2 + \Phi_2^\dagger \Phi_1) + \lambda_1 (\Phi_1^\dagger \Phi_1)^2 + \lambda_2 (\Phi_2^\dagger \Phi_2)^2 \\ & + 2\lambda_3 (\Phi_1^\dagger \Phi_1) (\Phi_2^\dagger \Phi_2) + 2\lambda_4 (\Phi_1^\dagger \Phi_2) (\Phi_2^\dagger \Phi_1) + \lambda_5 [(\Phi_1^\dagger \Phi_2)^2 + (\Phi_2^\dagger \Phi_1)^2]. \end{aligned} \quad (52)$$

The vacuum expectation values are

$$\langle \Phi_1 \rangle = \begin{pmatrix} 0 \\ e^{i\theta_1} v_1 / \sqrt{2} \end{pmatrix}, \quad \langle \Phi_2 \rangle = \begin{pmatrix} 0 \\ e^{i\theta_2} v_2 / \sqrt{2} \end{pmatrix}, \quad (53)$$

and break electroweak symmetry spontaneously. As anticipated in section 2, we use $\theta = \theta_2 - \theta_1$, $v^2 = v_1^2 + v_2^2$, $c_\beta = \cos \beta \equiv v_1/v$, $s_\beta = \sin \beta \equiv v_2/v$ and $t_\beta \equiv \tan \beta$, with $v_1 \geq 0$, $v_2 \geq 0$.

4.1 Minimization

The minimization conditions for $V(v_1, v_2, \theta) \equiv \mathcal{V}(\langle \Phi_1 \rangle, \langle \Phi_2 \rangle)$ are

$$\frac{\partial V}{\partial \theta} = -v_1 v_2 \sin \theta (\mu_{12}^2 + 2\lambda_5 v_1 v_2 \cos \theta) = 0, \quad (54)$$

$$\frac{\partial V}{\partial v_1} = \mu_{11}^2 v_1 + \lambda_1 v_1^3 + (\lambda_3 + \lambda_4) v_1 v_2^2 + v_2 (\mu_{12}^2 \cos \theta + \lambda_5 v_1 v_2 \cos 2\theta) = 0, \quad (55)$$

$$\frac{\partial V}{\partial v_2} = \mu_{22}^2 v_2 + \lambda_2 v_2^3 + (\lambda_3 + \lambda_4) v_1^2 v_2 + v_1 (\mu_{12}^2 \cos \theta + \lambda_5 v_1 v_2 \cos 2\theta) = 0. \quad (56)$$

In order to have spontaneous CP violation, we consider a solution $\{v_1, v_2, \theta\}$ of eqs. (54)–(56) with $\theta \neq 0, \pm\pi/2, \pm\pi$. From eq. (54) one obtains

$$\cos \theta = \frac{-\mu_{12}^2}{2\lambda_5 v_1 v_2}. \quad (57)$$

Notice that, in addition to θ , $-\theta$ is also a solution. It is obvious that for $\theta = 0, \pi$ the vacuum is CP invariant. It has also been shown [13] that for $\theta = \pi/2$ the vacuum is also CP invariant. Note from eq. (57) that $\theta = \pm\pi/2$ is obtained when $\mu_{12}^2 = 0$. In this case, the scalar potential is invariant under the \mathbb{Z}_2 symmetry of eq. (2). This symmetry allows the two scalar fields Φ_1, Φ_2 to have either equal or opposite CP parities. It is this freedom that is used to construct a simple proof [13] that for $\theta = \pm\pi/2$, the vacuum is CP invariant.

One can trade μ_{11}^2 , μ_{22}^2 and μ_{12}^2 for other parameters using eqs. (54)–(56):

$$\mu_{12}^2 = -2\lambda_5 v_1 v_2 \cos \theta, \quad (58)$$

$$\mu_{11}^2 = -(\lambda_1 v_1^2 + (\lambda_3 + \lambda_4 - \lambda_5) v_2^2), \quad (59)$$

$$\mu_{22}^2 = -(\lambda_2 v_2^2 + (\lambda_3 + \lambda_4 - \lambda_5) v_1^2). \quad (60)$$

That is, imposing eqs. (58)–(60) on $\mathcal{V}(\Phi_1, \Phi_2)$ in eq. (52), one is selecting a scalar potential where, at least, the necessary minimization conditions in eqs. (54)–(56) are satisfied for generic $\{v_1, v_2, \theta\}$. One can in addition choose $v_1^2 + v_2^2 = v^2 = (246 \text{ GeV})^2$ for appropriate electroweak symmetry breaking without loss of generality (this is enforced, for example, by a simple rescaling of the parameters in the potential). Fixing v^2 in that manner, one is left with a candidate minimum characterised by the values of θ and $\tan \beta = v_2/v_1$, which remain free parameters that we can choose at will, up to the different constraints on the scalar potential to be discussed later:

1. the potential is bounded from below and $V(v_1, v_2, \theta)$ is the lowest lying minimum;
2. perturbative unitarity bounds on scattering processes in the scalar sector are respected.

Expanding Φ_j around the candidate vacuum in eq. (53)

$$\Phi_j = e^{i\theta_j} \left(\frac{\varphi_j^+}{\sqrt{2}}(v_j + \rho_j + i\eta_j) \right), \quad (61)$$

we can now explore the different mass terms for the charged and neutral scalars. Requiring that the mass parameters of all the physical scalars are positive ensures, at least, that the candidate minimum is a local minimum of the potential. In the Higgs basis of eq. (5), the expansion of the fields reads

$$H_1 = \begin{pmatrix} G^+ \\ (v + H^0 + iG^0)/\sqrt{2} \end{pmatrix}, \quad H_2 = \begin{pmatrix} H^+ \\ (R^0 + iI^0)/\sqrt{2} \end{pmatrix}, \quad (62)$$

$$\begin{pmatrix} G^+ \\ H^+ \end{pmatrix} = \mathcal{R}_\beta \begin{pmatrix} \varphi_1^+ \\ \varphi_2^+ \end{pmatrix}, \quad \begin{pmatrix} G^0 \\ I^0 \end{pmatrix} = \mathcal{R}_\beta \begin{pmatrix} \eta_1 \\ \eta_2 \end{pmatrix}, \quad \begin{pmatrix} H^0 \\ R^0 \end{pmatrix} = \mathcal{R}_\beta \begin{pmatrix} \rho_1 \\ \rho_2 \end{pmatrix}, \quad (63)$$

with the would-be Goldstone bosons G^\pm and G^0 readily identified

$$G^\pm = c_\beta \varphi_1^\pm - s_\beta \varphi_2^\pm, \quad G^0 = c_\beta \eta_1 - s_\beta \eta_2. \quad (64)$$

4.2 Scalar masses and mixings

4.2.1 Charged scalar

The transformation into the Higgs basis also gives the mass term of the charged scalar $H^\pm = s_\beta \varphi_1^\pm - c_\beta \varphi_2^\pm$,

$$\mathcal{V}(\Phi_1, \Phi_2) \supset v^2(\lambda_5 - \lambda_4)H^+H^- \Rightarrow m_{H^\pm}^2 = v^2(\lambda_5 - \lambda_4). \quad (65)$$

Notice that, in order to choose a set of independent parameters, eq. (65) will allow us to trade λ_4 for $m_{H^\pm}^2$ and λ_5 . Furthermore, since λ_5 and λ_4 are subject to the constraints on the scalar potential discussed in appendix B, m_{H^\pm} has a limited allowed range: for example, if $\lambda_5 - \lambda_4 < 20$, then it follows that $m_{H^\pm} < 9m_h$.

4.2.2 Neutral scalars

For the neutral scalar sector, the mass terms are

$$\mathcal{V}(\Phi_1, \Phi_2) \supset \frac{1}{2} \begin{pmatrix} H^0 & R^0 & I^0 \end{pmatrix} \mathcal{M}_0^2 \begin{pmatrix} H^0 \\ R^0 \\ I^0 \end{pmatrix}, \quad (66)$$

with $\mathcal{M}_0^2 = \mathcal{M}_0^{2T}$, and

$$\begin{aligned} [\mathcal{M}_0^2]_{11} &= 2v^2 \{ \lambda_1 c_\beta^4 + \lambda_2 s_\beta^4 + 2c_\beta^2 s_\beta^2 [\lambda_{345} + 2\lambda_5 c_\theta^2] \}, \\ [\mathcal{M}_0^2]_{22} &= 2v^2 \{ c_\beta^2 s_\beta^2 (\lambda_1 + \lambda_2 - 2\lambda_{345}) + \lambda_5 (c_\beta^2 - s_\beta^2)^2 c_\theta^2 \}, \\ [\mathcal{M}_0^2]_{12} &= 2v^2 s_\beta c_\beta \{ -\lambda_1 c_\beta^2 + \lambda_2 s_\beta^2 + (c_\beta^2 - s_\beta^2) [\lambda_{345} + 2\lambda_5 c_\theta^2] \}, \\ [\mathcal{M}_0^2]_{13} &= -v^2 \lambda_5 s_{2\beta} s_{2\theta}, \\ [\mathcal{M}_0^2]_{23} &= -v^2 \lambda_5 c_{2\beta} s_{2\theta}, \\ [\mathcal{M}_0^2]_{33} &= 2v^2 \lambda_5 s_\theta^2, \end{aligned} \quad (67)$$

with, we recall, the shorthand notation $c_x = \cos x$, $s_x = \sin x$, and $\lambda_{345} \equiv \lambda_3 + \lambda_4 - \lambda_5$. For $\lambda_5 s_{2\theta} \neq 0$, attending to $[\mathcal{M}_0^2]_{13} \neq 0$ and $[\mathcal{M}_0^2]_{23} \neq 0$ above, there is scalar-pseudoscalar mixing, as it is expected from spontaneous breaking of CP in the scalar sector. \mathcal{M}_0^2 is diagonalised through a real orthogonal transformation \mathcal{R}

$$\mathcal{R}^T \mathcal{M}_0^2 \mathcal{R} = \text{diag}(m_h^2, m_H^2, m_A^2), \quad \mathcal{R}^{-1} = \mathcal{R}^T. \quad (68)$$

The physical neutral scalars are

$$\begin{pmatrix} h \\ H \\ A \end{pmatrix} = \mathcal{R}^T \begin{pmatrix} H^0 \\ R^0 \\ I^0 \end{pmatrix}, \quad (69)$$

and we assume h to be the lightest one, the Higgs-like neutral scalar with $m_h = 125$ GeV. With \mathcal{M}_0^2 in eqs. (67), \mathcal{R} ‘‘mixes’’, a priori, all three neutral scalars. It is interesting to notice that

$$\text{Tr}[\mathcal{M}_0^2] = m_h^2 + m_H^2 + m_A^2 = 2v^2 [\lambda_1 c_\beta^2 + \lambda_2 s_\beta^2 + \lambda_5], \quad (70)$$

and

$$\det[\mathcal{M}_0^2] = m_h^2 m_H^2 m_A^2 = 2v^6 \lambda_5 (\lambda_1 \lambda_2 - \lambda_{345}^2) \sin^2 2\beta \sin^2 \theta. \quad (71)$$

As explained in appendix B, since it is necessary that $\lambda_5 > 0$, it is also required that $\lambda_1 \lambda_2 > \lambda_{345}^2$ for $V(v_1, v_2, \theta)$ to be, at least, a local minimum (for which, necessarily, $\det[\mathcal{M}_0^2] > 0$).

Equations (70) and (71) encode in a transparent manner several interesting properties of the model. First, since the different λ_j are bounded by the requirements discussed in appendix B (in particular by perturbative unitarity), and $\sin^2 2\beta \leq 1$ and $\sin^2 \theta \leq 1$, the masses of the new scalars H , A , H^\pm , have a limited allowed range. For a very crude estimate, consider for example $\lambda_1 c_\beta^2 + \lambda_2 s_\beta^2 + \lambda_5 \sim 10$ in eq. (70): with $v \simeq 2m_h$,

$m_H^2 + m_A^2 \sim 80m_h^2$ and it is clear that the smaller among m_H and m_A cannot be larger than $\sim 6m_h$, while the larger among m_H and m_A cannot be larger than $\sim 9m_h$. On the other hand, from eq. (71), for $\sin 2\beta \ll 1$, at least one neutral scalar should be light and either $\tan \beta \gg 1$ or $\tan^{-1} \beta \gg 1$, which enhance SFCNC couplings. One can then expect that $\sin 2\beta \ll 1$ will be disfavoured by the constraints discussed in section 6, while $\tan \beta \sim \tan^{-1} \beta \sim 1$ are easier to accommodate. Finally, it is to be noticed that for $\sin \theta = 1$, there is no mixing among $\{h, H\}$ and A (and $m_A^2 = 2\lambda_5 v^2$), and, as discussed, no spontaneous CP violation and a real CKM matrix. For $\sin \theta = 0$, $m_A = 0$ and thus for $|\sin \theta| \ll 1$, one could expect again the presence of at least one light scalar.

From the previous comments, it emerges that in this model there is limited room to have a scalar sector where (i) h is a Higgs boson with quite SM-like properties and (ii) $m_{H^\pm}, m_H, m_A \gg m_h$. In this model, there is no decoupling regime for the new scalars. It is also clear, with these values, that the new scalars should be produced at the LHC. Nevertheless, the most relevant production and decay modes for their discovery will vary significantly between different regions of parameter space, including the Yukawa couplings discussed in section 5, and also the details of the lepton sector, and are thus beyond the scope of this work.

4.3 A simple analysis of the scalar sector

As a first step in the direction of the complete analysis of section 6, in this subsection we analyse the available parameter space of the scalar sector of the model, considering the following constraints.

- Agreement with electroweak precision data, in particular the oblique parameters S and T [23].
- Boundedness of the scalar potential and perturbative unitarity of the scattering processes, controlled by the scalar quartic couplings λ_j , as described, respectively, in appendices B.2 and B.3.
- We only consider $m_{H^\pm}, m_H, m_A \geq 150$ GeV; although masses of new scalars below 150 GeV are not automatically excluded by existing constraints, they would require specific analyses, interesting on their own, which are out of the scope of the present work. Furthermore, attending to eq. (71) and the related discussion, imposing this requirement on m_H and m_A translates into a *lower* bound on $s_{2\beta}^2$ and s_θ^2 . For a simple estimate one can take $\lambda_5(\lambda_1\lambda_2 - \lambda_{345}^2) < 10^2$, which gives (for $m_H, m_A \geq 150$ GeV) $s_{2\beta}^2, s_\theta^2 > 10^{-4}$. In terms of t_β , this means $10^{-2} < t_\beta < 10^2$. On the contrary, since the quantity relevant for the obtention of a realistic CKM matrix is $\sin 2\theta$ rather than $\sin \theta$, $s_\theta^2 > 10^{-4}$ is only relevant for $\theta \sim 0, \pi$, while $|\sin 2\theta| \ll 1$ with $\theta \sim \frac{\pi}{2}, \frac{3\pi}{2}$ is allowed.
- The analyses of Higgs signal strengths from the ATLAS and CMS collaborations, e.g. [24], put constraints on different couplings of h. Overall, the resulting picture corresponds to an h which is quite SM-like. For that reason, in order to discard

from this simple analysis the regions of parameter space that these constraints will in any case eliminate in the complete analysis of section 6, we require here $|\mathcal{R}_{11}| \geq 0.9$.

Although the analysis of section 3.4 already sets a lower bound $|\sin 2\theta| \geq 4 \times 10^{-3}$ in order to obtain the correct CKM matrix, we do not impose it here (it corresponds to the dashed vertical line in Figure 3(d)). A detailed discussion of one convenient parametrisation of all quantities related to the scalar sector is given in appendix B.1. With these ingredients, the allowed regions in Figures 3 and 4 are obtained. We introduce

$$M_{Min} \equiv \min(m_H, m_A, m_{H^\pm}), \quad M_{Max} \equiv \max(m_H, m_A, m_{H^\pm}). \quad (72)$$

Figure 3(a) shows that, with the simple requirements enumerated above, all new scalars cannot have, simultaneously, masses above ~ 750 GeV. These values are in rough agreement with the previous naive estimates. Figure 3(b) shows in addition that no new scalar can be heavier than ~ 950 GeV. It is also clear that the largest values of the scalar masses correspond to $t_\beta \simeq 1$, while only a reduced range of values of t_β is allowed, $10^{-1} < t_\beta < 10$. Figure 3(c) shows that the limitations on allowed M_{Min} and M_{Max} appear to be rather independent: for example, $M_{Max} \sim 850$ GeV is compatible with any value of M_{Min} below 750 GeV.

Figures 4(a)–4(c) illustrate that any ordering of the masses m_H, m_A, m_{H^\pm} is allowed, and no particular restriction arises besides the impossibility of having $m_H \simeq m_A > 250$ GeV.

Having introduced the physical scalars and analysed some relevant aspects of the scalar sector, we can now turn back to \mathcal{L}_Y in eq. (7) and discuss the Yukawa couplings of the physical quarks and scalars.

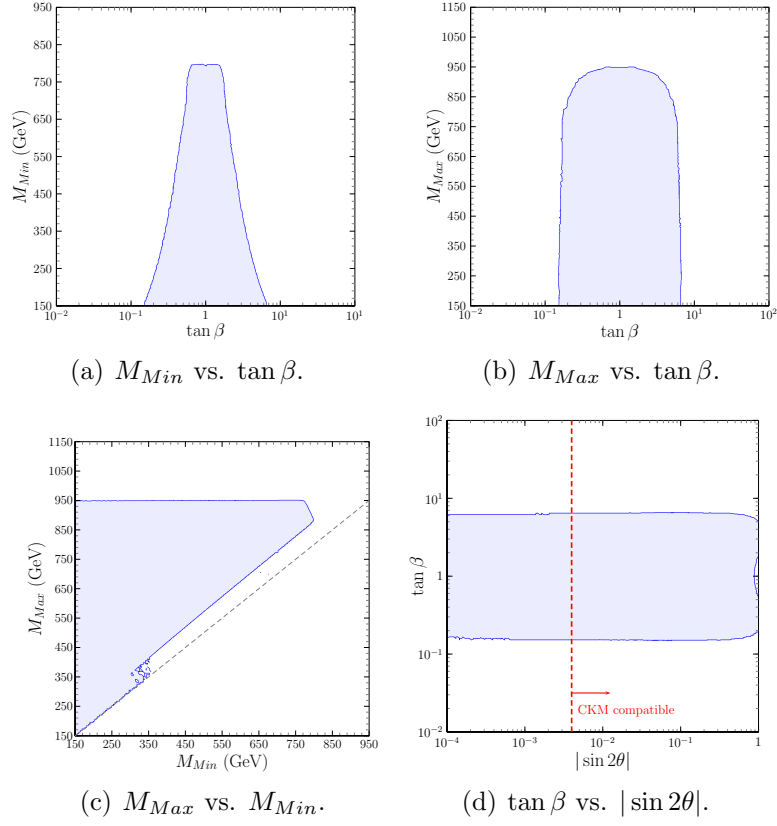


Figure 3: Regions allowed at 99% C.L. by the requirements on the scalar sector.

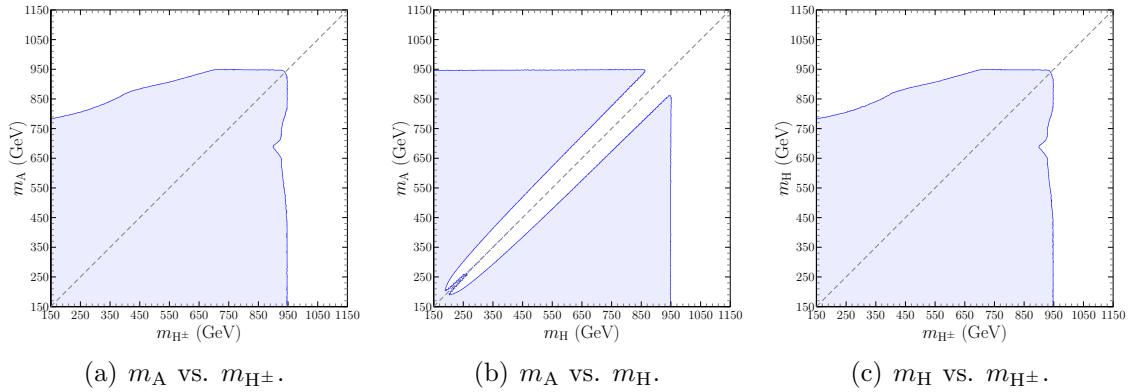


Figure 4: Regions allowed at 99% C.L. by the requirements on the scalar sector.

5 Physical Yukawa couplings

The Yukawa lagrangian in eq. (7)

$$\mathcal{L}_Y = \mathcal{L}_{\bar{q}q} + \mathcal{L}_{G\bar{q}q} + \mathcal{L}_{h\bar{q}q} + \mathcal{L}_{H\bar{q}q} + \mathcal{L}_{A\bar{q}q} + \mathcal{L}_{H^\pm\bar{q}q}, \quad (73)$$

gives the mass terms for quarks $\mathcal{L}_{\bar{q}q} = -\bar{d}_L M_d d_R - \bar{u}_L M_u u_R + \text{H.c.}$, the couplings to the would-be Goldstone bosons $\mathcal{L}_{G\bar{q}q}$,

$$\begin{aligned} \mathcal{L}_{G\bar{q}q} = & -i\frac{G^0}{v} [\bar{d}\gamma_5 d - \bar{u}\gamma_5 u] \\ & - \frac{\sqrt{2}G^+}{v} [\bar{u}_L V M_d d_R - \bar{u}_R M_u V d_L] - \frac{\sqrt{2}G^-}{v} [\bar{d}_R M_d V^\dagger u_L - \bar{d}_L V^\dagger M_u u_R], \end{aligned} \quad (74)$$

and the Yukawa couplings to the neutral and charged scalars $\mathcal{L}_{S\bar{q}q}$, $S = h, H, A, H^\pm$. Introducing the hermitian and antihermitian combinations

$$H_q \equiv \frac{N_q + N_q^\dagger}{2}, \quad A_q \equiv \frac{N_q - N_q^\dagger}{2}, \quad (75)$$

we have

$$\begin{aligned} \mathcal{L}_{S\bar{q}q} = & -\frac{S}{v} \left\{ \bar{d} [\mathcal{R}_{1s} M_d + \mathcal{R}_{2s} H_d + i\mathcal{R}_{3s} A_d] d + \bar{d} [\mathcal{R}_{2s} A_d + i\mathcal{R}_{3s} H_d] \gamma_5 d \right\} \\ & - \frac{S}{v} \left\{ \bar{u} [\mathcal{R}_{1s} M_u + \mathcal{R}_{2s} H_u - i\mathcal{R}_{3s} A_u] u + \bar{u} [\mathcal{R}_{2s} A_u - i\mathcal{R}_{3s} H_u] \gamma_5 u \right\}, \end{aligned} \quad (76)$$

with $s = 1, 2, 3$ for $S = h, H, A$, respectively, and

$$\mathcal{L}_{H^\pm\bar{q}q} = -\frac{\sqrt{2}H^+}{v} [\bar{u}_L V N_d d_R - \bar{u}_R N_u^\dagger V d_L] - \frac{\sqrt{2}H^-}{v} [\bar{d}_R N_d^\dagger V^\dagger u_L - \bar{d}_L V^\dagger N_u u_R]. \quad (77)$$

With eqs. (29)–(30), $[H_q]_{ij}$ and $[A_q]_{ij}$ in eq. (75) read

$$[H_q]_{ij} = t_\beta \delta_{ij} m_{q_i} - (t_\beta + t_\beta^{-1}) \hat{n}_{[q]i}^* \hat{n}_{[q]j} \frac{m_{d_i} + m_{d_j}}{2}, \quad (78)$$

$$[A_q]_{ij} = (t_\beta + t_\beta^{-1}) \hat{n}_{[q]i}^* \hat{n}_{[q]j} \frac{m_{d_i} - m_{d_j}}{2}. \quad (79)$$

We recall – see for example [25] – that, for flavour changing Yukawa couplings of quarks q_j, q_k and a scalar S , of the form

$$\mathcal{L}_{S q_j q_k} = -S \bar{q}_j (a_{jk} + i b_{jk} \gamma_5) q_k + \text{H.c.}, \quad a_{jk}, b_{jk} \in \mathbb{C}, \quad (80)$$

CP conservation requires $\text{Re}(a_{jk}^* b_{jk}) = 0$. In this model

$$\text{Re}(a_{jk}^* b_{jk}) \propto \mathcal{R}_{2s} \mathcal{R}_{3s} (t_\beta + t_\beta^{-1})^2 m_{q_j} m_{q_k} |\hat{n}_{[q]j}^* \hat{n}_{[q]k}|^2, \quad (81)$$

and thus, with \mathcal{R} mixing all three neutral scalars, the flavour changing Yukawa couplings are CP violating. For the charged scalar, we have

$$\text{Re}(a_{jk}^* b_{jk}) \propto \text{Im} \left((V N_d)_{jk}^* (N_u^\dagger V)_{jk} \right), \quad (82)$$

and thus in general, even for real N_q , the Yukawa couplings of H^\pm are also CP violating. For flavour conserving Yukawa couplings

$$\mathcal{L}_{\text{Sqq}} = -S\bar{q}(a + ib\gamma_5)q, \quad a, b \in \mathbb{R}, \quad (83)$$

CP conservation requires $ab = 0$. Then, for the coupling of the neutral scalar S , with eqs. (78)–(79), we have

$$ab \propto \mathcal{R}_{3s}m_{q_j}^2 (\mathcal{R}_{1s} + \mathcal{R}_{2s}[t_\beta - (t_\beta + t_\beta^{-1})|\hat{n}_{[q]j}|^2]) (t_\beta - (t_\beta + t_\beta^{-1})|\hat{n}_{[q]j}|^2), \quad (84)$$

and thus the flavour conserving Yukawa couplings violate CP as long as the mixing in the scalar sector connects A with h, H. Contributions to the electric dipole moment of the neutron arise from eq. (84), but the suppression due to the $m_{q_j}^2$ factor for $q_j = u, d$, together with the need of different non-zero mixings in the scalar sector, keep them within experimental bounds [26].

6 Phenomenology

6.1 Analysis and constraints

In section 3 we have shown that the model can give a CKM mixing matrix in agreement with data. We have also explored some aspects of the scalar sector in section 4. In this section we analyse the model considering simultaneously (i) obtention of an adequate CKM matrix (moduli $|V_{ij}|$ in the first and second rows and phase γ in agreement with data), (ii) a scalar sector verifying boundedness, perturbative unitarity, oblique parameter constraints and $m_H, m_A, m_{H^\pm} > 150$ GeV, and (iii) a number of constraints, to be discussed in the following, which involve both the quark Yukawa couplings and the scalar sector.

- Production \times decay signal strengths of the 125 GeV Higgs-like scalar h.
Agreement with the combined results of ATLAS and CMS from the LHC-Run I [24], together with additional data, involving in particular $h \rightarrow b\bar{b}$ [27, 28] from LHC-Run II, constrains the scalar mixings \mathcal{R}_{j1} and the diagonal entries of the N_d and N_u matrices (see, for example, [29]). Notice that the requirement $|\mathcal{R}_{11}| \geq 0.9$ used in section 4 to mimic coarsely the effect of these results is, of course, not imposed here.
- Neutral meson mixings.
One of the most relevant characteristics of the model is the presence of tree level flavour changing couplings of the neutral scalars: they produce the contributions to neutral meson mixing represented in Figure 5(a). They affect mass differences and CP violating observables [22, 30]. For $B_d^0-\bar{B}_d^0$ and $B_s^0-\bar{B}_s^0$ we impose agreement with the mass differences $\Delta M_{B_d}, \Delta M_{B_s}$ and the mixing \times decay CP asymmetries in $B_d \rightarrow J/\Psi K_S$ and $B_s \rightarrow J/\Psi \Phi$, respectively. For $K^0-\bar{K}^0$, we impose that the scalar mediated short distance contribution to M_{12}^K does not yield sizable contributions to ϵ_K and ΔM_K ; in particular, for ΔM_K , we require

$2|M_{12}^K|_{SFCNC} < \Delta M_K$. For $D^0-\bar{D}^0$, we impose, similarly, that the short distance contribution to M_{12}^D verifies $|M_{12}^D| < 3 \times 10^{-2} \text{ps}^{-1}$. In summary, neutral meson mixings constrain scalar mixings \mathcal{R}_{ij} and masses, together with off-diagonal entries of N_d and the 12, 21, elements of N_u .

Besides the SM one loop contribution, we only consider the scalar mediated tree level contributions to the Wilson coefficients of the different operators of interest; their QCD evolution from the electroweak scale to low energies follows [31–33]. For the operator matrix elements and bag factors, we use [34] and [35] (see also [36]).

- $b \rightarrow s\gamma$.

One loop diagrams like, for example, the ones in Figure 5(b), contribute to $\text{Br}(B \rightarrow X_s\gamma)$, and further constrain N_u and N_d , the neutral scalar mixings and masses, and m_{H^\pm} (in the previous constraints m_{H^\pm} does only appear in the one loop $h \rightarrow \gamma\gamma$ amplitude). Details of the calculation follow [37,38].

- Rare top decays $t \rightarrow hq$.

Current bounds [39–41] on $t \rightarrow hc, hu$ are at the 10^{-3} level, and have to be included in the analysis.

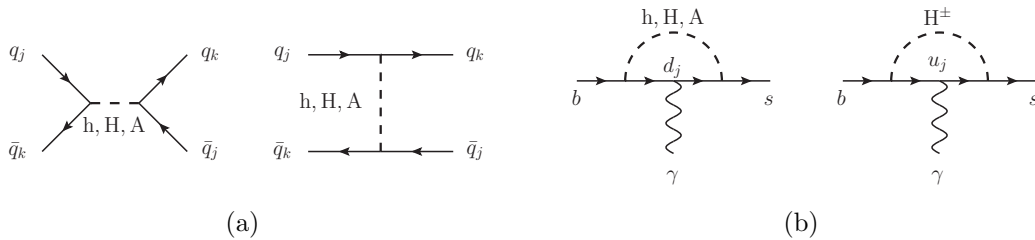


Figure 5: Diagrams contributing to: (a) meson mixing, (b) $b \rightarrow s\gamma$.

The analysis has two main goals:

1. to establish that the model is viable after a reasonable set of constraints is imposed;
2. to explore the prospects for the observation of some definite non-SM signal. We concentrate in particular on flavour changing decays $t \rightarrow hc, hu$ and $h \rightarrow bs, bd$, of interest, respectively, for the LHC and the ILC [42]. These are the most interesting tree level induced neutral flavour changing decays, since $h \rightarrow uc, ds$ are more suppressed by the light fermion mass factors in N_u and N_d (in addition, the experimental analysis is also more difficult having only light quarks in the final state).

We also consider a representative low energy observable, the time dependent CP violating asymmetry in $B_s \rightarrow J/\Psi\Phi$, $A_{J/\Psi\Phi}^{CP}$, for which the SM prediction is $A_{J/\Psi\Phi}^{CP} \simeq -0.04$, while current results [43] give -0.030 ± 0.033 , leaving significant room for New Physics contributions.

Further implications for the phenomenology of H , A and H^\pm , vary significantly between allowed regions in the parameter space of the model (for example, the relevant decay modes change depending on which scalar is heavier and on the values of the N_q matrices), and would also involve, and be sensitive to, the couplings of the scalars with leptons, which we have not discussed in this work. As commented in precedence, we do not address such implications here. The fact that we have not included a description of the leptonic sector prevents (i) the use of constraints such as, for example, $\text{Br}(B_s \rightarrow \mu^+ \mu^-)$ or $\text{Br}(K_L \rightarrow \mu^+ \mu^-)$, and (ii) considerations on potential New Physics signals which involve leptons, as the so-called ‘‘B anomalies’’ [44].

6.2 Results

The main results of the full analysis are presented in Figures 6 to 11.

Figure 6(a) corresponds to Figures 2(d)–2(f) of the analysis in section 3: as one could anticipate, it is to be noticed that the allowed regions, where the model satisfies all the constraints, are much reduced with respect to the simple requirement of section 3, i.e. just reproducing a realistic CKM matrix. In particular, the only allowed regions for θ_d and φ_d correspond to having one component of $\hat{r}_{[d]}$ close to ± 1 (that is close to the points $(0, \pm 1)$, $(\pm 1, 0)$, $(0, 0)$ in Figure 6(a)), and the remaining two components much smaller: this naturally suppresses neutral flavour changing couplings, since they depend on the products of different components. As discussed in subsection 3.2 and in appendix A, *without actually reaching that exact point*, at which the CKM matrix becomes CP conserving. From this point of view, those regions are ‘‘close to’’ (but not exactly) the different types of BGL models (as discussed in [12]), in which (i) tree SFCNC are absent in one of the quark sectors and (ii) the scalar potential does not permit spontaneous CP violation. This is clearly illustrated by Figures 6(d), 6(e) and 6(f), that are enlargements of Figure 6(a) with peculiar logarithmic scales where values below 10^{-3} have been collapsed to the central point. These central points correspond, respectively, to the flavour structures of the BGL models of types d , s and b . For example, the b BGL model corresponds to $\hat{r}_{[d]} = (0, 0, \pm 1)$. The figures show that the allowed regions exclude the BGL models, but remain close. Correspondingly, the regions close to the flavour structures of up type BGL models (which are also indicated in the Figures), remain empty, i.e. they are not allowed. For example, the t BGL model corresponds to the small holes in the allowed region in Figure 6(f).

Figures 6(b) and 6(c) correspond to Figures 2(b) and 2(c) in subsection 3.4: the range of allowed values for $|\hat{r}_{[d]Mid}|$, $|\hat{r}_{[u]Mid}|$ is reduced in the full analysis, in particular the largest allowed values are now smaller than 0.3.

Figure 7 corresponds to Figure 3 of the analysis of the scalar sector in section 4. It is clear that the constraints of the full analysis reduce the available room for t_β , leaving only $1/4 < t_\beta < 4$. Furthermore, the allowed region in M_{Max} vs. M_{Min} in Fig. 7(c) is slightly reduced with respect to Fig. 3(c). Notice in particular that the region with all new scalars light, i.e. $M_{Max} < 250$ GeV, is now almost excluded. On the contrary, the largest values of M_{Max} and M_{Min} coincide with those in section 4, that is, they are still limited by the requirements on the scalar sector itself. The same comments apply to Figure 8, which corresponds to Figure 4 of the analysis of section 4. Notice that

$|\sin 2\theta|$ is now required to be in the range $[0.03; 1.0]$.

Figure 9(a) shows that deviations from $|\mathcal{R}_{11}| = 1$ can be achieved for almost all values of t_β within the allowed range, while Figures 9(b) and 9(c) illustrate, as expected, that for large values of $|\sin 2\theta|$, \mathcal{R}_{31} (which controls the amount of pseudoscalar I^0 entering h), reaches the larger allowed values, while $|\mathcal{R}_{11}|$ is reduced. Notice in particular that, overall, $|\mathcal{R}_{31}| \geq 10^{-2}$ and that values as large as $|\mathcal{R}_{31}| \sim 0.4$ are allowed. In any case, even if $|\mathcal{R}_{11}|$ can reach values very close to 1, $|\mathcal{R}_{11}| < 1$.

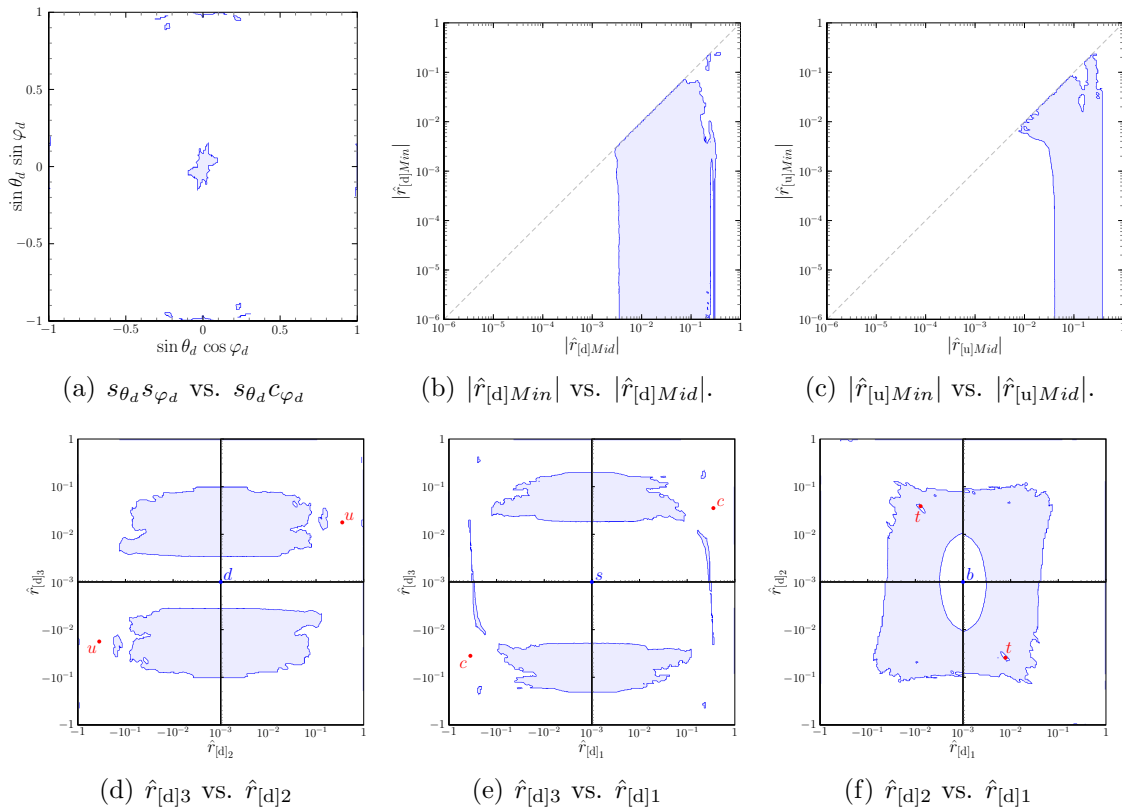


Figure 6: Regions allowed at 99% C.L. by the requirements of the full analysis.

Finally, Figures 10 and 11 illustrate some New Physics prospects in different flavour changing neutral transitions.

Figure 10(a) shows⁹ $\text{Br}(h \rightarrow bs)$ vs. $A_{J/\Psi\Phi}^{CP}$; it is interesting to notice that: (i) $\text{Br}(h \rightarrow bs)$ can reach values as large as 10^{-2} , relevant for searches at the ILC, and (ii) significant deviations of the SM expectation $A_{J/\Psi\Phi}^{CP} \simeq -0.036$ can arise. An interesting correlation among New Physics effects follows: $A_{J/\Psi\Phi}^{CP}$ values neatly different from SM expectations (the dashed vertical line in Figure 10(a)) would necessarily require values of $\text{Br}(h \rightarrow bs)$ in the range 10^{-4} - 10^{-2} . The origin of such a correlation is clear: the tree level couplings that induce $h \rightarrow bs$ at that level also contribute significantly to the dispersive amplitude $M_{12}^{B_s}$ in $B_s^0 - \bar{B}_s^0$ mixing, changing its phase while maintaining $|M_{12}^{B_s}|$ (i.e. ΔM_{B_s}). According to the discussion on the connection of SFCNC and CP violation in

⁹The notation is $\text{Br}(h \rightarrow bs) \equiv \text{Br}(h \rightarrow \bar{b}s + b\bar{s})$, $\text{Br}(h \rightarrow bd) \equiv \text{Br}(h \rightarrow \bar{b}d + b\bar{d})$, etc.

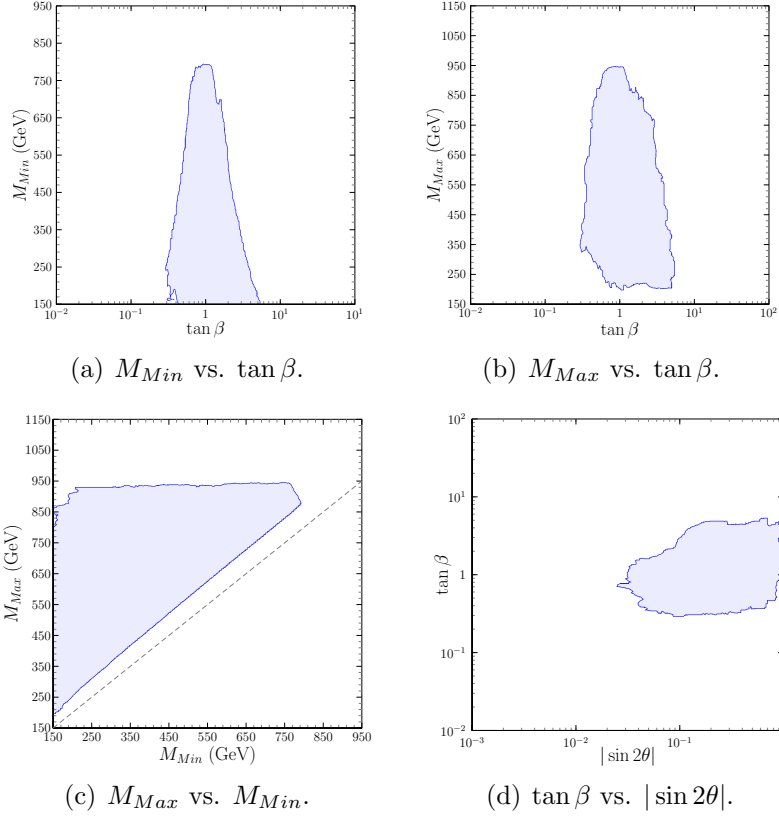


Figure 7: Regions allowed at 99% C.L. by the requirements of the full analysis.

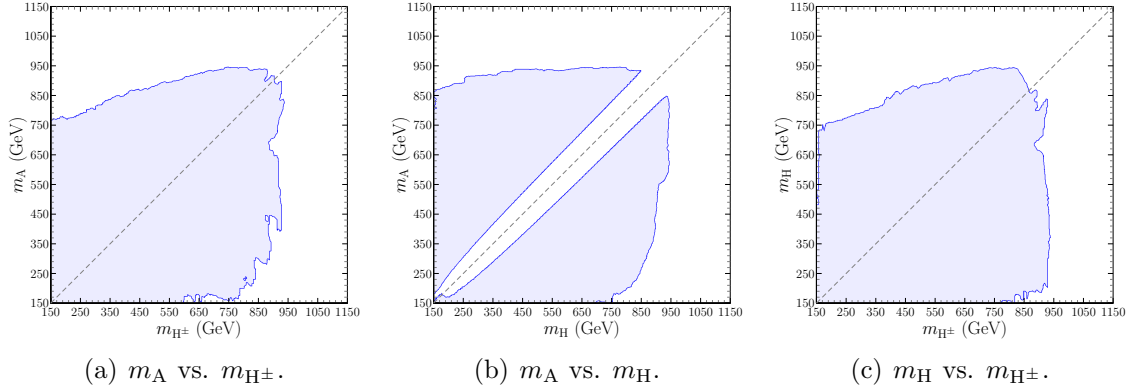


Figure 8: Regions allowed at 99% C.L. by the requirements of the full analysis.

subsection 3.2, tree level SFCNC should give

$$\begin{aligned}
 \text{Br}(t \rightarrow hc) + \text{Br}(t \rightarrow hu) + \text{Br}(h \rightarrow cu) &\neq 0 & \text{and} \\
 \text{Br}(h \rightarrow bs) + \text{Br}(h \rightarrow bd) + \text{Br}(h \rightarrow sd) &\neq 0.
 \end{aligned}
 \tag{85}$$

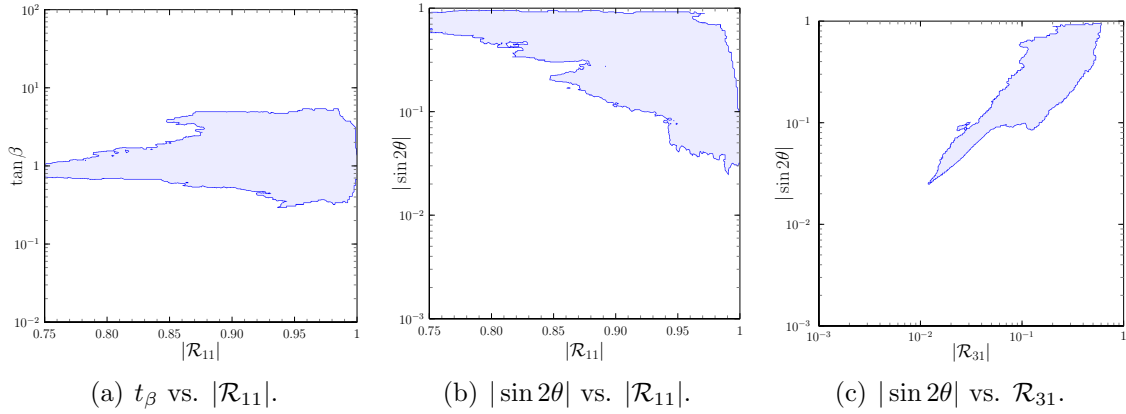


Figure 9: Regions allowed at 99% C.L. by the requirements of the full analysis.

We introduce

$$\begin{aligned}
 \text{Br}(t \rightarrow hq) &\equiv \text{Br}(t \rightarrow hc) + \text{Br}(t \rightarrow hu), \\
 \text{Br}(h \rightarrow bq) &\equiv \text{Br}(h \rightarrow bs) + \text{Br}(h \rightarrow bd), \\
 \text{Br}(h \rightarrow q_1 q_2) &\equiv \text{Br}(h \rightarrow bq) + \text{Br}(h \rightarrow sd) + \text{Br}(h \rightarrow cu).
 \end{aligned} \tag{86}$$

Concentrating on the decays of h , eq. (85) implies, for the total rate of flavour changing decays of h $\text{Br}(h \rightarrow q_1 q_2)$, $\text{Br}(h \rightarrow q_1 q_2) \neq 0$. Figure 10(b) clearly shows that in any case $5 \times 10^{-6} \leq \text{Br}(h \rightarrow q_1 q_2) \leq 2 \times 10^{-2}$.

Figure 11 shows different correlations among the branching ratios of flavour changing transitions involving h . It is important to notice that these New Physics signals are not confined to one particular sector (up or down type quarks) and that the largest allowed rates can be achieved for the transitions with second and third generation quarks, $t \rightarrow hc$ and $h \rightarrow bs$. Notice in particular that for $t \rightarrow hc$, the LHC bounds at the level of 10^{-3} do play a role in limiting the allowed regions. Of course, the remaining transitions, $t \rightarrow hu$ and $h \rightarrow bd, sd, cu$ are also interesting: even if the largest values of their rates are smaller than the largest values allowed for $t \rightarrow hc$ and $h \rightarrow bs$, in some regions of the parameter space they have larger rates than $t \rightarrow hc$ and $h \rightarrow bs$, and they can also be within experimental reach.

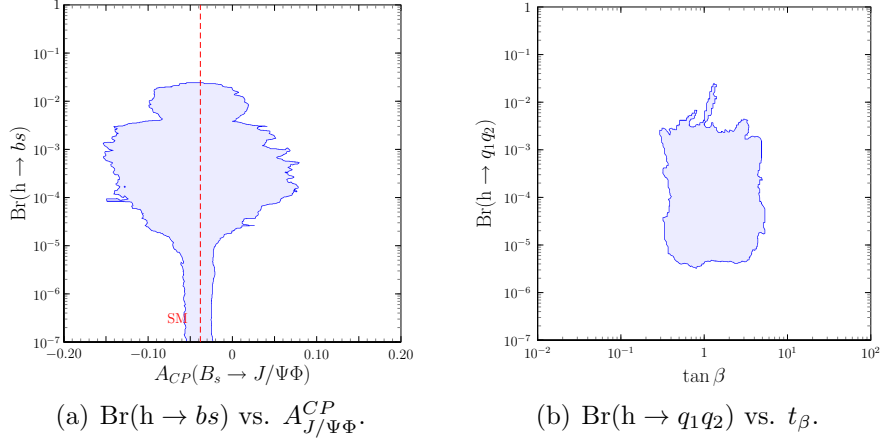


Figure 10: Region allowed at 99% C.L. by the requirements of the full analysis.

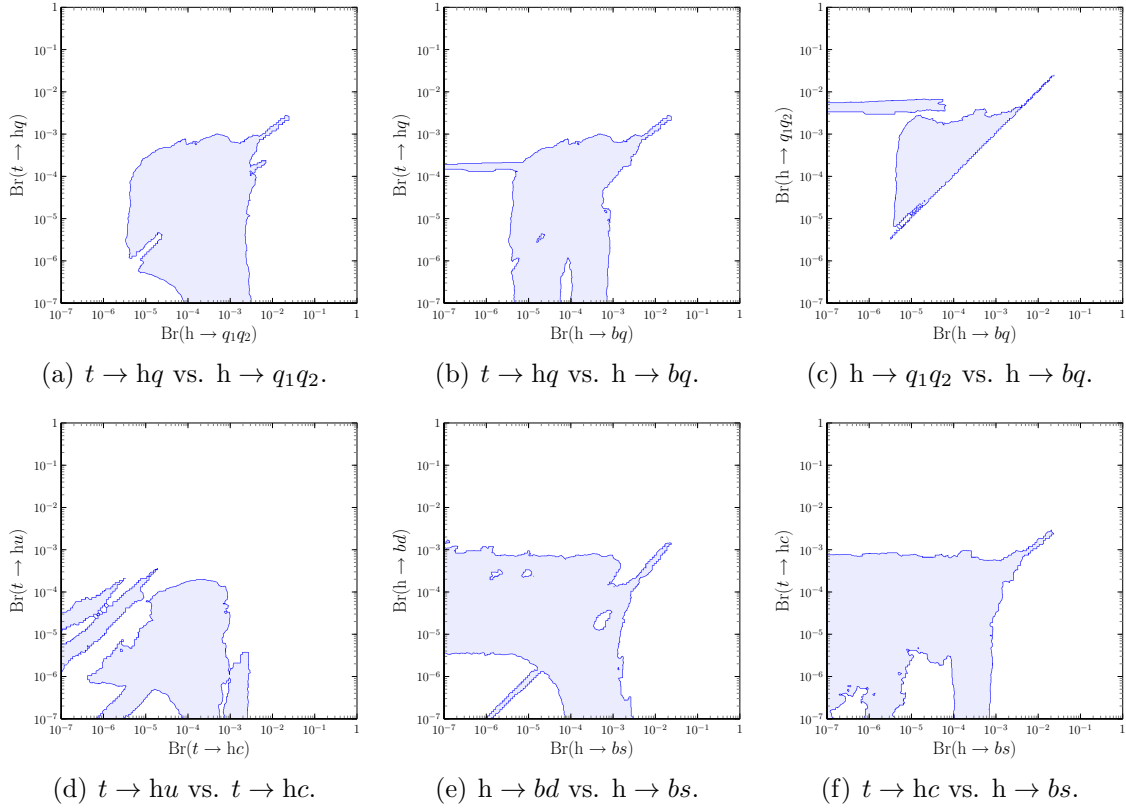


Figure 11: Regions allowed at 99% C.L. by the requirements of the full analysis.

Conclusions

In this paper we have addressed the question: is it possible to construct a realistic model with spontaneous CP violation, in the framework of a minimal two Higgs doublet extension of the Standard Model? We show that this is indeed possible. In order to accomplish this task, one has to surmount enormous obstacles, like having a natural suppression of SFCNC and generating a complex CKM matrix from the vacuum phase, with the correct strength of the invariant measure of the amount of CP violation in the quark mixing matrix.

We have shown that a minimal scenario is phenomenological viable, through the introduction of a flavoured \mathbb{Z}_2 symmetry, where one of the three quark families is odd under \mathbb{Z}_2 while the other two are even. A remarkable feature of the model is its prediction of New Physics which can be discovered at the LHC. More precisely, the model predicts that all the new scalars have a mass below 950 GeV with at least one of the masses below 750 GeV. This prediction is obtained through a thorough study of the constraints arising from the 125 GeV Higgs signals, the size of neutral meson mixings, the size of $b \rightarrow s\gamma$, and reproducing a correct CKM matrix, including the size of CP violation. Constraints from the electroweak oblique parameters, and perturbative unitarity and boundedness of the scalar potential are also included.

We encounter a deep connection between the generation of a complex CKM matrix from a vacuum phase and the necessary appearance of SFCNC. In the New Physics predictions, we give special emphasis to processes like $t \rightarrow hc, hu, h \rightarrow bs, bd$, which are relevant for the LHC and the ILC. Interestingly, there is still room for important New Physics contributions to the phase of $B_s^0-\bar{B}_s^0$ mixing.

In the present model of SCPV, none of the new scalars can be heavier than 1 TeV, and the presence of SFCNC cannot be avoided. The experimental constraints select regions in parameter space where the SFCNC are kept under control, as happens in BGL models. It is indeed remarkable that these allowed regions are located close to BGL models: for example, in the neighbourhood of a down-type BGL flavour structure, we almost do not have SFCNC in the down sector while the SFCNC in the up sector are of the Minimal Flavour Violating type [6]. Apparently these are the only regions within this model, where one can have an effective suppression of the dangerous SFCNC.

Acknowledgments

This work is partially supported by Spanish MINECO under grant FPA2017-85140-C3-3-P and by the Severo Ochoa Excellence Center Project SEV-2014-0398, by Generalitat Valenciana under grant GVPROMETEOII 2014-049 and by Fundação para a Ciência e a Tecnologia (FCT, Portugal) through the projects CERN/FIS-NUC/0010/2015 CFTP-FCT Unit 777 (UID/FIS/00777/2013) and PTDC/FIS-PAR/29436/2017 which are partially funded through POCTI (FEDER), COMPETE, QREN and EU. MN acknowledges support from FCT through postdoctoral grant SFRH/BPD/112999/2015.

A SFCNC and CP Violating CKM

In subsection 3.2 we have addressed the incompatibility between a CP violating CKM matrix and the absence of tree level SFCNC in one quark sector, in this model. In this appendix we provide a simple proof that completes the discussion.

Let us consider the case of the down quark sector. According to eqs. (22) and (23),

$$N_d = [t_\beta \mathbf{1} - (t_\beta + t_\beta^{-1}) \mathcal{O}_L^{dT} \mathbf{P}_3 \mathcal{O}_L^d] M_d, \quad [\mathcal{O}_L^{dT} \mathbf{P}_3 \mathcal{O}_L^d]_{ij} = \hat{r}_{[d]i} \hat{r}_{[d]j}. \quad (87)$$

Tree level SFCNC in the down sector are absent when $\mathcal{O}_L^{dT} \mathbf{P}_3 \mathcal{O}_L^d$ is diagonal, that is $\hat{r}_{[d]i} = \delta_{ik}$ for some k (1 or 2 or 3). In that case,

$$[\mathcal{O}_L^{dT} \mathbf{P}_3 \mathcal{O}_L^d]_{ij} = \delta_{ik} \delta_{jk} = \delta_{ik} \delta_{ij} = [\mathbf{P}_k]_{ij} \quad (88)$$

with the projectors

$$\mathbf{P}_1 = \begin{pmatrix} 1 & 0 & 0 \\ 0 & 0 & 0 \\ 0 & 0 & 0 \end{pmatrix}, \quad \mathbf{P}_2 = \begin{pmatrix} 0 & 0 & 0 \\ 0 & 1 & 0 \\ 0 & 0 & 0 \end{pmatrix}, \quad \mathbf{P}_3 = \begin{pmatrix} 0 & 0 & 0 \\ 0 & 0 & 0 \\ 0 & 0 & 1 \end{pmatrix}. \quad (89)$$

On the other hand, the CKM matrix in eq. (33) reads in that case

$$V = \mathcal{O}_L^{uT} [\mathbf{1} + (e^{i2\theta} - 1) \mathbf{P}_3] \mathcal{O}_L^d = R [\mathbf{1} + (e^{i2\theta} - 1) \mathcal{O}_L^{dT} \mathbf{P}_3 \mathcal{O}_L^d] = R [\mathbf{1} + (e^{i2\theta} - 1) \mathbf{P}_k], \quad (90)$$

it is the product of a real orthogonal matrix R and a diagonal matrix of phases, and hence CP conserving.

For the up quark sector, the reasoning is analogous: the absence of tree level SFCNC requires $\mathcal{O}_L^{uT} \mathbf{P}_3 \mathcal{O}_L^u$ to be diagonal in

$$N_u = [t_\beta \mathbf{1} - (t_\beta + t_\beta^{-1}) \mathcal{O}_L^{uT} \mathbf{P}_3 \mathcal{O}_L^u] M_u, \quad [\mathcal{O}_L^{uT} \mathbf{P}_3 \mathcal{O}_L^u]_{ij} = \hat{r}_{[u]i} \hat{r}_{[u]j}, \quad (91)$$

that is $\hat{r}_{[u]i} = \delta_{ik}$ for some k , in which case $[\mathcal{O}_L^{uT} \mathbf{P}_3 \mathcal{O}_L^u]_{ij} = [\mathbf{P}_k]_{ij}$ and

$$V = [\mathbf{1} + (e^{i2\theta} - 1) \mathcal{O}_L^{uT} \mathbf{P}_3 \mathcal{O}_L^u] R = [\mathbf{1} + (e^{i2\theta} - 1) \mathbf{P}_k] R, \quad (92)$$

with the CKM matrix the product of a diagonal matrix of phases and a real orthogonal matrix R , hence CP conserving again.

B Scalar potential

In this appendix we discuss different aspects concerning the scalar potential of section 4: in B.1 the election of a convenient set of basic parameters, in B.2 boundedness (from below) of the potential, then perturbativity requirements in B.3, and finally, in B.4, a simple proof that $\lambda_5 > 0$ is a necessary condition in the present scenario.

B.1 Independent parameters

It is important to discuss the number and nature of the independent parameters of interest in the scalar sector. The goal is to adopt the most convenient choice for them. Through the minimization conditions of section 4.1, it is already clear that one can trade the three quadratic coefficients μ_{ij}^2 for v^2 , β and θ , and set $v = 246$ GeV. At this stage one could already consider a set of values for $\{\lambda_j\}$, $j = 1, \dots, 5$, compute m_{H^\pm} , the mass matrix \mathcal{M}_0^2 , and from \mathcal{M}_0^2 , obtain, at least numerically, m_h^2 , m_H^2 , m_A^2 and the mixings \mathcal{R} . Of course, one would then need to impose appropriate conditions: for example $m_h^2 > 0$, $m_H^2 > 0$, $m_A^2 > 0$. This is hardly the most convenient strategy, since, besides the computational toll, one would like for example to impose $m_h = 125$ GeV. The phenomenological conditions in section 6.1 can be imposed afterwards. With this in mind, one would prefer to have (beside β and θ), m_h^2 , m_H^2 , m_A^2 , $m_{H^\pm}^2$ and three angles α_j describing \mathcal{R} as parameters, and the different λ_j expressed in terms of them.

We have already noticed that λ_4 can be traded for $m_{H^\pm}^2$ and λ_5 using eq. (65); this leaves *four* quantities, λ_1 , λ_2 , λ_{345} and λ_5 , that, together with β and θ , determine \mathcal{M}_0^2 (i.e. six different matrix elements). On the other hand, in \mathcal{M}_0^2 , we have three masses, m_h^2 , m_H^2 , m_A^2 , while \mathcal{R} requires three parameters: *six* quantities. It is to be expected that they cannot be chosen independently. One simple procedure that can be adopted is the following:

1. equating elements $[\mathcal{M}_0^2]_{13}$, $[\mathcal{M}_0^2]_{23}$ and $[\mathcal{M}_0^2]_{33}$ in eqs. (67) with their expressions in terms of m_h^2 , m_H^2 , m_A^2 , and \mathcal{R} , they can be read as a linear system in λ_5 , m_H^2 , m_A^2 which can be solved, giving them in terms of m_h^2 , \mathcal{R} and of course β , v^2 and θ ;
2. then, equating elements $[\mathcal{M}_0^2]_{11}$, $[\mathcal{M}_0^2]_{22}$ and $[\mathcal{M}_0^2]_{12}$ in eqs. (67) with their expressions in terms of m_h^2 , m_H^2 , m_A^2 , and \mathcal{R} , they can be read as a linear system in λ_1 , λ_2 and λ_{345} , which can also be solved, giving them in terms of m_h^2 , \mathcal{R} , β , v^2 and θ ;
3. λ_4 is simply given by $\lambda_4 = \lambda_5 - m_{H^\pm}^2/v^2$ with λ_5 already known;
4. with λ_{345} , λ_4 and λ_5 known, λ_3 is trivially $\lambda_3 = \lambda_{345} + \lambda_5 - \lambda_4$.

Summarising: with these simple steps, for given values of β , v^2 , θ , m_h^2 , $m_{H^\pm}^2$ and \mathcal{R} (three α_j), one can compute m_H^2 , m_A^2 and all λ_j , $j = 1$ to 5. For that set of values to be acceptable, one should then require

- positive values of all masses (m_h^2 and $m_{H^\pm}^2$ can be chosen and thus only $m_H^2 > 0$ and $m_A^2 > 0$ have to be checked),
- boundedness from below of $\mathcal{V}(\Phi_1, \Phi_2)$ and absolute minimum for $\{v^2, \beta, \theta\}$,
- perturbative unitarity requirements on λ 's.

In order to illustrate the procedure to express m_A^2 , m_H^2 and all λ_j in terms of the basic set of parameters $\{v^2, \beta, \theta, m_h^2, m_{H^\pm}^2, \alpha_j\}$, we start with the use of $[\mathcal{M}_0^2]_{13}$, $[\mathcal{M}_0^2]_{23}$ and

$[\mathcal{M}_0^2]_{33}$ to obtain m_A^2 , m_H^2 and λ_5 . One needs to equate those elements in eqs. (67) to

$$[\mathcal{M}_0^2]_{13} = m_h^2 \mathcal{R}_{11} \mathcal{R}_{31} + m_H^2 \mathcal{R}_{12} \mathcal{R}_{32} + m_A^2 \mathcal{R}_{13} \mathcal{R}_{33}, \quad (93)$$

$$[\mathcal{M}_0^2]_{23} = m_h^2 \mathcal{R}_{21} \mathcal{R}_{31} + m_H^2 \mathcal{R}_{22} \mathcal{R}_{32} + m_A^2 \mathcal{R}_{23} \mathcal{R}_{33}, \quad (94)$$

$$[\mathcal{M}_0^2]_{33} = m_h^2 \mathcal{R}_{31}^2 + m_H^2 \mathcal{R}_{32}^2 + m_A^2 \mathcal{R}_{33}^2. \quad (95)$$

From the orthonormality relations $(\mathcal{R}^T \mathcal{R})_{ij} = \delta_{ij}$ we have

$$m_h^2 \mathcal{R}_{31} = \mathcal{R}_{11} [\mathcal{M}_0^2]_{13} + \mathcal{R}_{21} [\mathcal{M}_0^2]_{23} + \mathcal{R}_{31} [\mathcal{M}_0^2]_{33}, \quad (96)$$

$$m_H^2 \mathcal{R}_{32} = \mathcal{R}_{12} [\mathcal{M}_0^2]_{13} + \mathcal{R}_{22} [\mathcal{M}_0^2]_{23} + \mathcal{R}_{32} [\mathcal{M}_0^2]_{33}, \quad (97)$$

$$m_A^2 \mathcal{R}_{33} = \mathcal{R}_{13} [\mathcal{M}_0^2]_{13} + \mathcal{R}_{23} [\mathcal{M}_0^2]_{23} + \mathcal{R}_{33} [\mathcal{M}_0^2]_{33}, \quad (98)$$

and thus

$$m_h^2 \mathcal{R}_{31} = v^2 \lambda_5 [-s_{2\beta} s_{2\theta} \mathcal{R}_{11} - c_{2\beta} s_{2\theta} \mathcal{R}_{21} + 2s_\theta^2 \mathcal{R}_{31}], \quad (99)$$

$$m_H^2 = m_h^2 \frac{\mathcal{R}_{31} \mathcal{R}_{12} [\mathcal{M}_0^2]_{13} + \mathcal{R}_{22} [\mathcal{M}_0^2]_{23} + \mathcal{R}_{32} [\mathcal{M}_0^2]_{33}}{\mathcal{R}_{32} \mathcal{R}_{11} [\mathcal{M}_0^2]_{13} + \mathcal{R}_{21} [\mathcal{M}_0^2]_{23} + \mathcal{R}_{31} [\mathcal{M}_0^2]_{33}}, \quad (100)$$

$$m_A^2 = m_h^2 \frac{\mathcal{R}_{31} \mathcal{R}_{13} [\mathcal{M}_0^2]_{13} + \mathcal{R}_{23} [\mathcal{M}_0^2]_{23} + \mathcal{R}_{33} [\mathcal{M}_0^2]_{33}}{\mathcal{R}_{33} \mathcal{R}_{11} [\mathcal{M}_0^2]_{13} + \mathcal{R}_{21} [\mathcal{M}_0^2]_{23} + \mathcal{R}_{31} [\mathcal{M}_0^2]_{33}}. \quad (101)$$

The solution reads

$$\lambda_5 = \frac{m_h^2 \mathcal{R}_{31}}{2v^2} \frac{1}{s_\theta s_\beta \mathcal{R}_{31} - c_\theta c_{2\beta} \mathcal{R}_{21} - c_\theta s_{2\beta} \mathcal{R}_{11}}, \quad (102)$$

$$m_H^2 = m_h^2 \frac{\mathcal{R}_{31}}{\mathcal{R}_{32}} \left[\frac{-c_\theta s_{2\beta} \mathcal{R}_{12} - c_\theta c_{2\beta} \mathcal{R}_{22} + s_\theta \mathcal{R}_{32}}{-c_\theta s_{2\beta} \mathcal{R}_{11} - c_\theta c_{2\beta} \mathcal{R}_{21} + s_\theta \mathcal{R}_{31}} \right], \quad (103)$$

$$m_A^2 = m_h^2 \frac{\mathcal{R}_{31}}{\mathcal{R}_{33}} \left[\frac{-c_\theta s_{2\beta} \mathcal{R}_{13} - c_\theta c_{2\beta} \mathcal{R}_{23} + s_\theta \mathcal{R}_{33}}{-c_\theta s_{2\beta} \mathcal{R}_{11} - c_\theta c_{2\beta} \mathcal{R}_{21} + s_\theta \mathcal{R}_{31}} \right]. \quad (104)$$

Next, equating elements $[\mathcal{M}_0^2]_{11}$, $[\mathcal{M}_0^2]_{22}$ and $[\mathcal{M}_0^2]_{12}$ in eqs. (67) to

$$[\mathcal{M}_0^2]_{11} = m_h^2 \mathcal{R}_{11}^2 + m_H^2 \mathcal{R}_{12}^2 + m_A^2 \mathcal{R}_{13}^2, \quad (105)$$

$$[\mathcal{M}_0^2]_{22} = m_h^2 \mathcal{R}_{21}^2 + m_H^2 \mathcal{R}_{22}^2 + m_A^2 \mathcal{R}_{23}^2, \quad (106)$$

$$[\mathcal{M}_0^2]_{12} = m_h^2 \mathcal{R}_{11} \mathcal{R}_{21} + m_H^2 \mathcal{R}_{12} \mathcal{R}_{22} + m_A^2 \mathcal{R}_{13} \mathcal{R}_{23}, \quad (107)$$

one can solve for λ_1 , λ_2 and λ_{345} :

$$\lambda_1 = \frac{1}{2v^2} [[\mathcal{M}_0^2]_{11} + t_\beta^2 [\mathcal{M}_0^2]_{22} + 2t_\beta [\mathcal{M}_0^2]_{12}] - \lambda_5 c_\theta^2 t_\beta^2, \quad (108)$$

$$\lambda_2 = \frac{1}{2v^2} [[\mathcal{M}_0^2]_{11} + t_\beta^{-2} [\mathcal{M}_0^2]_{22} - 2t_\beta^{-1} [\mathcal{M}_0^2]_{12}] - \lambda_5 c_\theta^2 t_\beta^{-2}, \quad (109)$$

$$\lambda_{345} = \frac{1}{2v^2} [[\mathcal{M}_0^2]_{11} - [\mathcal{M}_0^2]_{22} + (t_\beta^{-1} - t_\beta) [\mathcal{M}_0^2]_{12}] - \lambda_5 c_\theta^2, \quad (110)$$

that is

$$\lambda_1 = \frac{m_h^2}{2v^2}(\mathcal{R}_{11} - t_\beta \mathcal{R}_{21})^2 + \frac{m_H^2}{2v^2}(\mathcal{R}_{12} - t_\beta \mathcal{R}_{22})^2 + \frac{m_A^2}{2v^2}(\mathcal{R}_{13} - t_\beta \mathcal{R}_{23})^2 - \lambda_5 c_\theta^2 t_\beta^2, \quad (111)$$

$$\lambda_2 = \frac{m_h^2}{2v^2}(\mathcal{R}_{11} + t_\beta^{-1} \mathcal{R}_{21})^2 + \frac{m_H^2}{2v^2}(\mathcal{R}_{12} + t_\beta^{-1} \mathcal{R}_{22})^2 + \frac{m_A^2}{2v^2}(\mathcal{R}_{13} + t_\beta^{-1} \mathcal{R}_{23})^2 - \lambda_5 c_\theta^2 t_\beta^{-2}, \quad (112)$$

$$\begin{aligned} \lambda_{345} &= \frac{m_h^2}{2v^2}(\mathcal{R}_{11}^2 - \mathcal{R}_{21}^2 + (t_\beta^{-1} - t_\beta)\mathcal{R}_{11}\mathcal{R}_{21}) + \frac{m_H^2}{2v^2}(\mathcal{R}_{12}^2 - \mathcal{R}_{22}^2 + (t_\beta^{-1} - t_\beta)\mathcal{R}_{12}\mathcal{R}_{22}) \\ &\quad + \frac{m_A^2}{2v^2}(\mathcal{R}_{13}^2 - \mathcal{R}_{23}^2 + (t_\beta^{-1} - t_\beta)\mathcal{R}_{13}\mathcal{R}_{23}) - \lambda_5 c_\theta^2, \end{aligned} \quad (113)$$

with m_H^2 , m_A^2 and λ_5 in eqs.(102)–(104). To complete the procedure, we just need to recall

$$\lambda_4 = \lambda_5 - m_{H^\pm}^2/v^2, \quad \lambda_3 = \lambda_{345} - \lambda_4 + \lambda_5. \quad (114)$$

B.2 Boundedness and absolute minimum

The conditions to be imposed on the resulting λ_j 's for a scalar potential bounded from below are

$$\lambda_1 > 0, \quad \lambda_2 > 0, \quad \sqrt{\lambda_1 \lambda_2} > -\lambda_3, \quad \lambda_{345} > -\sqrt{\lambda_1 \lambda_2}. \quad (115)$$

Notice that with the expression of $\det \mathcal{M}_0^2$ in eq.(71), with $\lambda_5 > 0$ (see subsection B.4 below) it follows from $\det \mathcal{M}_0^2 > 0$ that

$$\sqrt{\lambda_1 \lambda_2} > \lambda_{345} > -\sqrt{\lambda_1 \lambda_2}. \quad (116)$$

One last concern on the scalar potential is the possibility that the local minimum for $\{v^2, \beta, \theta\}$ is not the absolute minimum of the potential, but instead a metastable minimum which can decay to the “true” absolute minimum (such a situation is sometimes dubbed the *panic vacuum* [45]). From general studies of the minimization problem in 2HDM [45–48], it follows that $\{v^2, \beta, \theta\}$ and $\{v^2, \beta, -\theta\}$ (this discrete ambiguity arised already in eq.(57)) give indeed the absolute minima of the potential.

B.3 Perturbative unitarity

Requiring perturbative unitarity of tree level scattering processes translates into the following bounds [49, 50] (one loop corrections in a CP conserving 2HDM scenario have

been addressed in [51])

$$\begin{aligned}
\lambda_1 + \lambda_2 \pm \sqrt{(\lambda_1 - \lambda_2)^2 + 4\lambda_5^2} &< \Lambda, \\
2(\lambda_3 + \lambda_4) &< \Lambda, \\
2(\lambda_3 - \lambda_4) &< \Lambda, \\
\lambda_1 + \lambda_2 \pm \sqrt{(\lambda_1 - \lambda_2)^2 + 4\lambda_4^2} &< \Lambda, \\
2(\lambda_3 \pm \lambda_5) &< \Lambda, \\
3(\lambda_1 + \lambda_2) \pm \sqrt{9(\lambda_1 - \lambda_2)^2 + 4(2\lambda_3 + \lambda_4)^2} &< \Lambda, \\
2(\lambda_3 + 2\lambda_4 \pm 3\lambda_5) &< \Lambda,
\end{aligned} \tag{117}$$

with $\Lambda = 16\pi$.

B.4 $\lambda_5 > 0$

As anticipated in section 4, the necessary condition $\lambda_5 > 0$ follows from a simple requirement on the scalar potential. If $V(v_1, v_2, \theta)$ is the absolute minimum of the potential, it is obviously necessary that $V(v_1, v_2, \theta) < V(v_1, v_2, 0)$ and $V(v_1, v_2, \theta) < V(v_1, v_2, \pi)$. Notice that, although $\{v_1, v_2, 0\}$ and $\{v_1, v_2, \pi\}$ fulfill eq. (54), they do not fulfill eqs. (55)–(56), that is, V cannot have a minimum for $\{v_1, v_2, 0\}$, $\{v_1, v_2, \pi\}$. Since the θ -independent terms of V are common to all three cases, we only need to analyse the θ -dependent part, V_θ .

$$V_\theta(v_1, v_2, \frac{0}{\pi}) = v_1 v_2 \left[\pm \mu_{12}^2 + \frac{1}{2} v_1 v_2 \lambda_5 \right] = v_1^2 v_2^2 \lambda_5 \left[\frac{1}{2} \mp 2 \cos \theta \right], \tag{118}$$

while

$$V_\theta(v_1, v_2, \theta) = v_1 v_2 \left[\mu_{12}^2 \cos \theta + \frac{1}{2} v_1 v_2 \lambda_5 (2 \cos^2 \theta - 1) \right] = -v_1^2 v_2^2 \lambda_5 \left[\cos^2 \theta + \frac{1}{2} \right]. \tag{119}$$

Then

$$\begin{aligned}
V_\theta(v_1, v_2, \theta) < V_\theta(v_1, v_2, \frac{0}{\pi}) &\Leftrightarrow \\
-v_1^2 v_2^2 \lambda_5 \left[\cos^2 \theta + \frac{1}{2} \right] < v_1^2 v_2^2 \lambda_5 \left[\frac{1}{2} \mp 2 \cos \theta \right] &\Leftrightarrow -\lambda_5 (1 \mp \cos \theta)^2 < 0,
\end{aligned} \tag{120}$$

that is $\lambda_5 > 0$.

C Rephasings

The diagonalisation of the mass matrices M_d^0 and M_u^0 is only defined up to rephasings of the quark mass eigenstates. With

$$M_d = \text{diag}(m_{d_j}) = \mathcal{U}_L^{d\dagger} M_d^0 \mathcal{U}_R^d, \quad M_u = \text{diag}(m_{u_j}) = \mathcal{U}_L^{u\dagger} M_u^0 \mathcal{U}_R^u, \tag{121}$$

and the rephasings

$$R_d = \text{diag}(e^{i\varphi_j^d}), R_u = \text{diag}(e^{i\varphi_j^u}), \quad R_q^\dagger = R_q^{-1} = R_q^*, \quad (122)$$

it is clear that

$$R_d^\dagger M_d R_d = M_d = \mathcal{U}_L^{d\dagger} M_d^0 \mathcal{U}_R^d, \quad R_u^\dagger M_u R_u = M_u = \mathcal{U}_L^{u\dagger} M_u^0 \mathcal{U}_R^u. \quad (123)$$

Consequently the diagonalising unitary matrices \mathcal{U}_L^d , \mathcal{U}_L^u , \mathcal{U}_R^d and \mathcal{U}_R^u are only given up to common redefinitions

$$\mathcal{U}_L^d \mapsto \mathcal{U}_L^d R_d, \quad \mathcal{U}_R^d \mapsto \mathcal{U}_R^d R_d, \quad \mathcal{U}_L^u \mapsto \mathcal{U}_L^u R_u, \quad \mathcal{U}_R^u \mapsto \mathcal{U}_R^u R_u. \quad (124)$$

Under such rephasings, the CKM matrix is transformed into

$$V \mapsto R_u^\dagger V R_d, \quad V_{jk} \mapsto e^{i(\varphi_k^d - \varphi_j^u)} V_{jk}. \quad (125)$$

The off-diagonal elements of the matrices N_d and N_u are also transformed under rephasings,

$$N_d \mapsto R_d^\dagger N_d R_d, \quad N_u \mapsto R_u^\dagger N_u R_u, \quad (126)$$

with

$$\hat{n}_{[d]j} = [\mathcal{U}_L^d]_{3j} \mapsto [\mathcal{U}_L^d R_d]_{3j} = e^{i\varphi_j^d} \hat{n}_{[d]j}, \quad \hat{n}_{[d]j}^* \hat{n}_{[d]k} \mapsto e^{i(\varphi_k^d - \varphi_j^d)} \hat{n}_{[d]j}^* \hat{n}_{[d]k}, \quad (127)$$

and

$$\hat{n}_{[u]j} = [\mathcal{U}_L^u]_{3j} \mapsto [\mathcal{U}_L^u R_u]_{3j} = e^{i\varphi_j^u} \hat{n}_{[u]j}, \quad \hat{n}_{[u]j}^* \hat{n}_{[u]k} \mapsto e^{i(\varphi_k^u - \varphi_j^u)} \hat{n}_{[u]j}^* \hat{n}_{[u]k}. \quad (128)$$

References

- [1] T. Lee, *A Theory of Spontaneous T Violation*, *Phys.Rev.* **D8** (1973) 1226–1239.
- [2] G. Branco, P. Ferreira, L. Lavoura, M. Rebelo, M. Sher, *et al.*, *Theory and phenomenology of two-Higgs-doublet models*, *Phys.Rept.* **516** (2012) 1–102, [1106.0034].
- [3] I. P. Ivanov, *Building and testing models with extended Higgs sectors*, *Prog. Part. Nucl. Phys.* **95** (2017) 160–208, [1702.03776].
- [4] S. L. Glashow and S. Weinberg, *Natural Conservation Laws for Neutral Currents*, *Phys.Rev.* **D15** (1977) 1958.
- [5] G. Branco, W. Grimus, and L. Lavoura, *Relating the scalar flavor changing neutral couplings to the CKM matrix*, *Phys.Lett.* **B380** (1996) 119–126, [hep-ph/9601383].
- [6] F. Botella, G. Branco, and M. Rebelo, *Minimal Flavour Violation and Multi-Higgs Models*, *Phys.Lett.* **B687** (2010) 194–200, [0911.1753].
- [7] F. Botella, G. Branco, M. Nebot, and M. Rebelo, *Two-Higgs Leptonic Minimal Flavour Violation*, *JHEP* **1110** (2011) 037, [1102.0520].
- [8] G. Bhattacharyya, D. Das, and A. Kundu, *Feasibility of light scalars in a class of two-Higgs-doublet models and their decay signatures*, *Phys.Rev.* **D89** (2014) 095029, [1402.0364].
- [9] F. Botella, G. Branco, A. Carmona, M. Nebot, L. Pedro, and M. Rebelo, *Physical Constraints on a Class of Two-Higgs Doublet Models with FCNC at tree level*, *JHEP* **1407** (2014) 078, [1401.6147].
- [10] A. Celis, J. Fuentes-Martin, and H. Serodio, *An invisible axion model with controlled FCNCs at tree level*, *Phys. Lett.* **B741** (2015) 117–123, [1410.6217].
- [11] F. J. Botella, G. C. Branco, M. Nebot, and M. N. Rebelo, *Flavour Changing Higgs Couplings in a Class of Two Higgs Doublet Models*, *Eur. Phys. J.* **C76** (2016), no. 3 161, [1508.05101].
- [12] J. M. Alves, F. J. Botella, G. C. Branco, F. Cornet-Gomez, and M. Nebot, *Controlled Flavour Changing Neutral Couplings in Two Higgs Doublet Models*, *Eur. Phys. J.* **C77** (2017), no. 9 585, [1703.03796].
- [13] G. C. Branco, *Spontaneous CP Nonconservation and Natural Flavor Conservation: A Minimal Model*, *Phys. Rev.* **D22** (1980) 2901.
- [14] G. C. Branco and M. N. Rebelo, *The Higgs Mass in a Model With Two Scalar Doublets and Spontaneous CP Violation*, *Phys. Lett.* **B160** (1985) 117–120.

- [15] G. C. Branco and I. P. Ivanov, *Group-theoretic restrictions on generation of CP-violation in multi-Higgs-doublet models*, *JHEP* **01** (2016) 116, [1511.02764].
- [16] F. Botella, G. Branco, M. Nebot, and M. Rebelo, *New physics and evidence for a complex CKM*, *Nucl.Phys.* **B725** (2005) 155–172, [hep-ph/0502133].
- [17] H. Georgi and D. V. Nanopoulos, *Suppression of Flavor Changing Effects From Neutral Spinless Meson Exchange in Gauge Theories*, *Phys. Lett.* **B82** (1979) 95.
- [18] J. F. Donoghue and L. F. Li, *Properties of Charged Higgs Bosons*, *Phys. Rev.* **D19** (1979) 945.
- [19] F. J. Botella and J. P. Silva, *Jarlskog - like invariants for theories with scalars and fermions*, *Phys. Rev.* **D51** (1995) 3870–3875, [hep-ph/9411288].
- [20] P. M. Ferreira, L. Lavoura, and J. P. Silva, *A Soft origin for CKM-type CP violation*, *Phys. Lett.* **B704** (2011) 179–188, [1102.0784].
- [21] G. C. Branco, *Spontaneous CP Violation in Theories with More Than Four Quarks*, *Phys. Rev. Lett.* **44** (1980) 504.
- [22] **Particle Data Group** Collaboration, C. Patrignani *et al.*, *Review of Particle Physics*, *Chin. Phys.* **C40** (2016), no. 10 100001.
- [23] W. Grimus, L. Lavoura, O. Ogreid, and P. Osland, *The Oblique parameters in multi-Higgs-doublet models*, *Nucl.Phys.* **B801** (2008) 81–96, [0802.4353].
- [24] **ATLAS, CMS** Collaboration, G. Aad *et al.*, *Measurements of the Higgs boson production and decay rates and constraints on its couplings from a combined ATLAS and CMS analysis of the LHC pp collision data at $\sqrt{s} = 7$ and 8 TeV*, *JHEP* **08** (2016) 045, [1606.02266].
- [25] M. Nebot and J. P. Silva, *Self-cancellation of a scalar in neutral meson mixing and implications for the LHC*, *Phys. Rev.* **D92** (2015), no. 8 085010, [1507.07941].
- [26] M. Jung and A. Pich, *Electric Dipole Moments in Two-Higgs-Doublet Models*, *JHEP* **04** (2014) 076, [1308.6283].
- [27] **ATLAS** Collaboration, M. Aaboud *et al.*, *Evidence for the $H \rightarrow b\bar{b}$ decay with the ATLAS detector*, *JHEP* **12** (2017) 024, [1708.03299].
- [28] **CMS** Collaboration, A. M. Sirunyan *et al.*, *Evidence for the Higgs boson decay to a bottom quark-antiquark pair*, 1709.07497.
- [29] F. J. Botella, F. Cornet-Gomez, and M. Nebot, *Flavour Conservation in Two Higgs Doublet Models*, 1803.08521.
- [30] **Heavy Flavor Averaging Group (HFAG)** Collaboration, Y. Amhis *et al.*, *Averages of b-hadron, c-hadron, and τ -lepton properties as of summer 2014*, 1412.7515.

- [31] M. Ciuchini, E. Franco, V. Lubicz, G. Martinelli, I. Scimemi, and L. Silvestrini, *Next-to-leading order QCD corrections to Delta F = 2 effective Hamiltonians*, *Nucl. Phys.* **B523** (1998) 501–525, [[hep-ph/9711402](#)].
- [32] A. J. Buras, M. Misiak, and J. Urban, *Two loop QCD anomalous dimensions of flavor changing four quark operators within and beyond the standard model*, *Nucl. Phys.* **B586** (2000) 397–426, [[hep-ph/0005183](#)].
- [33] J. Aebischer, M. Fael, C. Greub, and J. Virto, *B physics Beyond the Standard Model at One Loop: Complete Renormalization Group Evolution below the Electroweak Scale*, *JHEP* **09** (2017) 158, [[1704.06639](#)].
- [34] **ETM** Collaboration, N. Carrasco, P. Dimopoulos, R. Frezzotti, V. Lubicz, G. C. Rossi, S. Simula, and C. Tarantino, *$\Delta S = 2$ and $\Delta C = 2$ bag parameters in the standard model and beyond from $N_f=2+1+1$ twisted-mass lattice QCD*, *Phys. Rev.* **D92** (2015), no. 3 034516, [[1505.06639](#)].
- [35] **Fermilab Lattice, MILC** Collaboration, A. Bazavov *et al.*, *$B_{(s)}^0$ -mixing matrix elements from lattice QCD for the Standard Model and beyond*, *Phys. Rev.* **D93** (2016), no. 11 113016, [[1602.03560](#)].
- [36] S. Aoki *et al.*, *Review of lattice results concerning low-energy particle physics*, *Eur. Phys. J.* **C77** (2017), no. 2 112, [[1607.00299](#)].
- [37] M. Misiak *et al.*, *Estimate of $\mathcal{B}(\bar{B} \rightarrow X_s \gamma)$ at $O(\alpha_s^2)$* , *Phys. Rev. Lett.* **98** (2007) 022002, [[hep-ph/0609232](#)].
- [38] A. Crivellin, A. Kokulu, and C. Greub, *Flavor-phenomenology of two-Higgs-doublet models with generic Yukawa structure*, *Phys.Rev.* **D87** (2013), no. 9 094031, [[1303.5877](#)].
- [39] **ATLAS** Collaboration, M. Aaboud *et al.*, *Search for top quark decays $t \rightarrow qH$, with $H \rightarrow \gamma\gamma$, in $\sqrt{s} = 13$ TeV pp collisions using the ATLAS detector*, *JHEP* **10** (2017) 129, [[1707.01404](#)].
- [40] **CMS** Collaboration, V. Khachatryan *et al.*, *Search for top quark decays via Higgs-boson-mediated flavor-changing neutral currents in pp collisions at $\sqrt{s} = 8$ TeV*, *JHEP* **02** (2017) 079, [[1610.04857](#)].
- [41] **CMS** Collaboration, A. M. Sirunyan *et al.*, *Search for the flavor-changing neutral current interactions of the top quark and the Higgs boson which decays into a pair of b quarks at $\sqrt{s} = 13$ TeV*, [1712.02399](#).
- [42] D. Barducci and A. J. Helmboldt, *Quark flavour-violating Higgs decays at the ILC*, *JHEP* **12** (2017) 105, [[1710.06657](#)].
- [43] **HFLAV** Collaboration, Y. Amhis *et al.*, *Averages of b-hadron, c-hadron, and τ -lepton properties as of summer 2016*, *Eur. Phys. J.* **C77** (2017), no. 12 895, [[1612.07233](#)].

- [44] J. Albrecht, S. Reichert, and D. van Dyk, *Status of rare exclusive B meson decays in 2018*, 1806.05010.
- [45] I. P. Ivanov and J. P. Silva, *Tree-level metastability bounds for the most general two Higgs doublet model*, *Phys. Rev.* **D92** (2015), no. 5 055017, [1507.05100].
- [46] I. P. Ivanov, *Minkowski space structure of the Higgs potential in 2HDM. II. Minima, symmetries, and topology*, *Phys. Rev.* **D77** (2008) 015017, [0710.3490].
- [47] A. Barroso, P. M. Ferreira, I. P. Ivanov, R. Santos, and J. P. Silva, *Evading death by vacuum*, *Eur. Phys. J.* **C73** (2013) 2537, [1211.6119].
- [48] A. Barroso, P. M. Ferreira, I. P. Ivanov, and R. Santos, *Metastability bounds on the two Higgs doublet model*, *JHEP* **06** (2013) 045, [1303.5098].
- [49] S. Kanemura, T. Kubota, and E. Takasugi, *Lee-Quigg-Thacker bounds for Higgs boson masses in a two doublet model*, *Phys. Lett.* **B313** (1993) 155–160, [hep-ph/9303263].
- [50] I. F. Ginzburg and I. P. Ivanov, *Tree-level unitarity constraints in the most general 2HDM*, *Phys. Rev.* **D72** (2005) 115010, [hep-ph/0508020].
- [51] B. Grinstein, C. W. Murphy, and P. Uttayarat, *One-loop corrections to the perturbative unitarity bounds in the CP-conserving two-Higgs doublet model with a softly broken \mathbb{Z}_2 symmetry*, *JHEP* **06** (2016) 070, [1512.04567].